Physics-based Integration of H2-Air Rotating Detonation into Gas Turbine Power Plant (HydrogenGT)

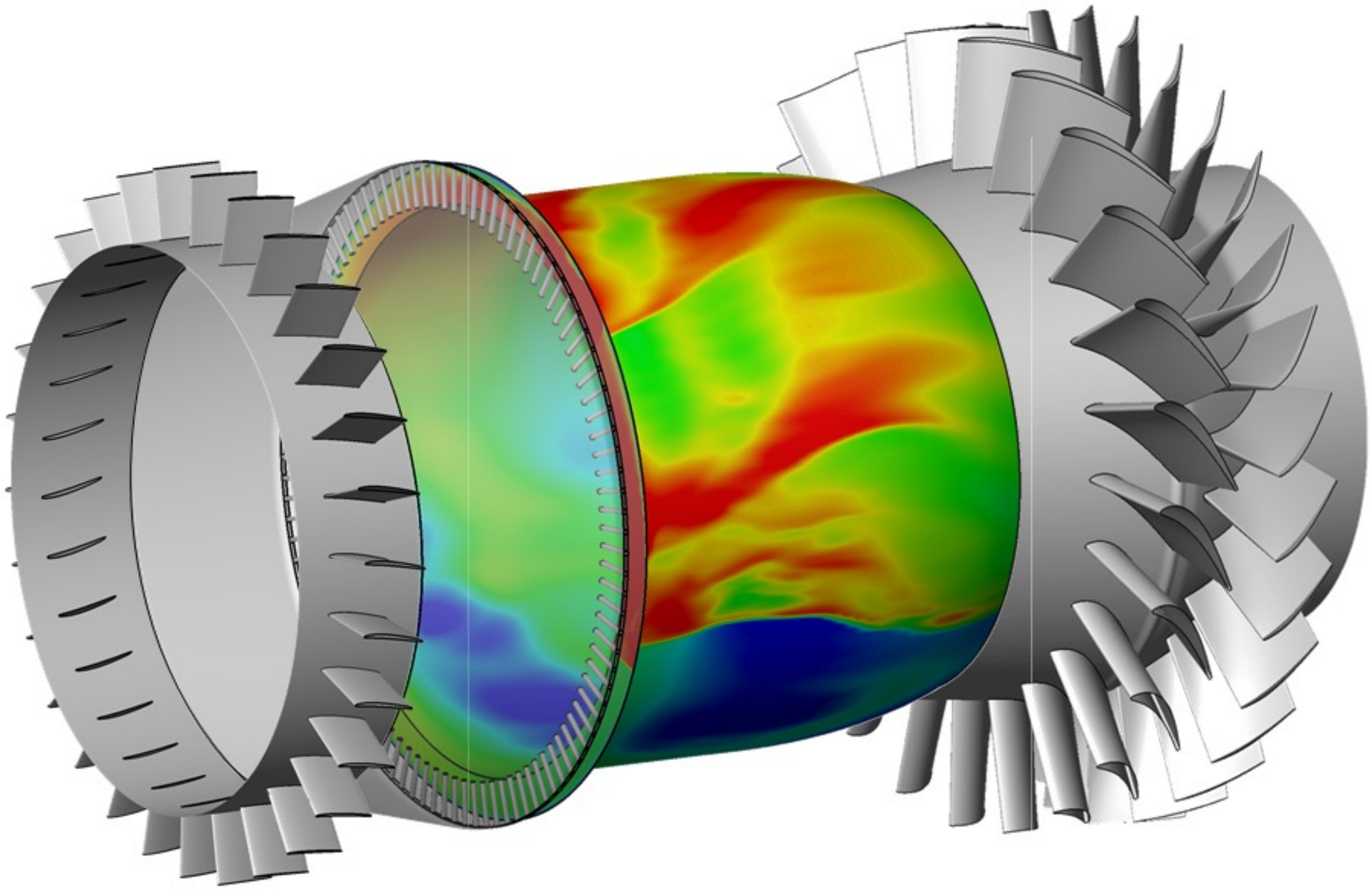

PI: Guillermo, gpaniagua@purdue.edu
Co-PI: James, braun26@purdue.edu
Co-PI: Terry, trmeyer@purdue.edu
Co-PI: Pinaki, pal@anl.gov
Co-PI: Carson, cslabau@purdue.edu

develop a high-speed diffuser-turbine from rotating detonation combustors (RDC) to industrial turbines

Turbomachinery II - ME533

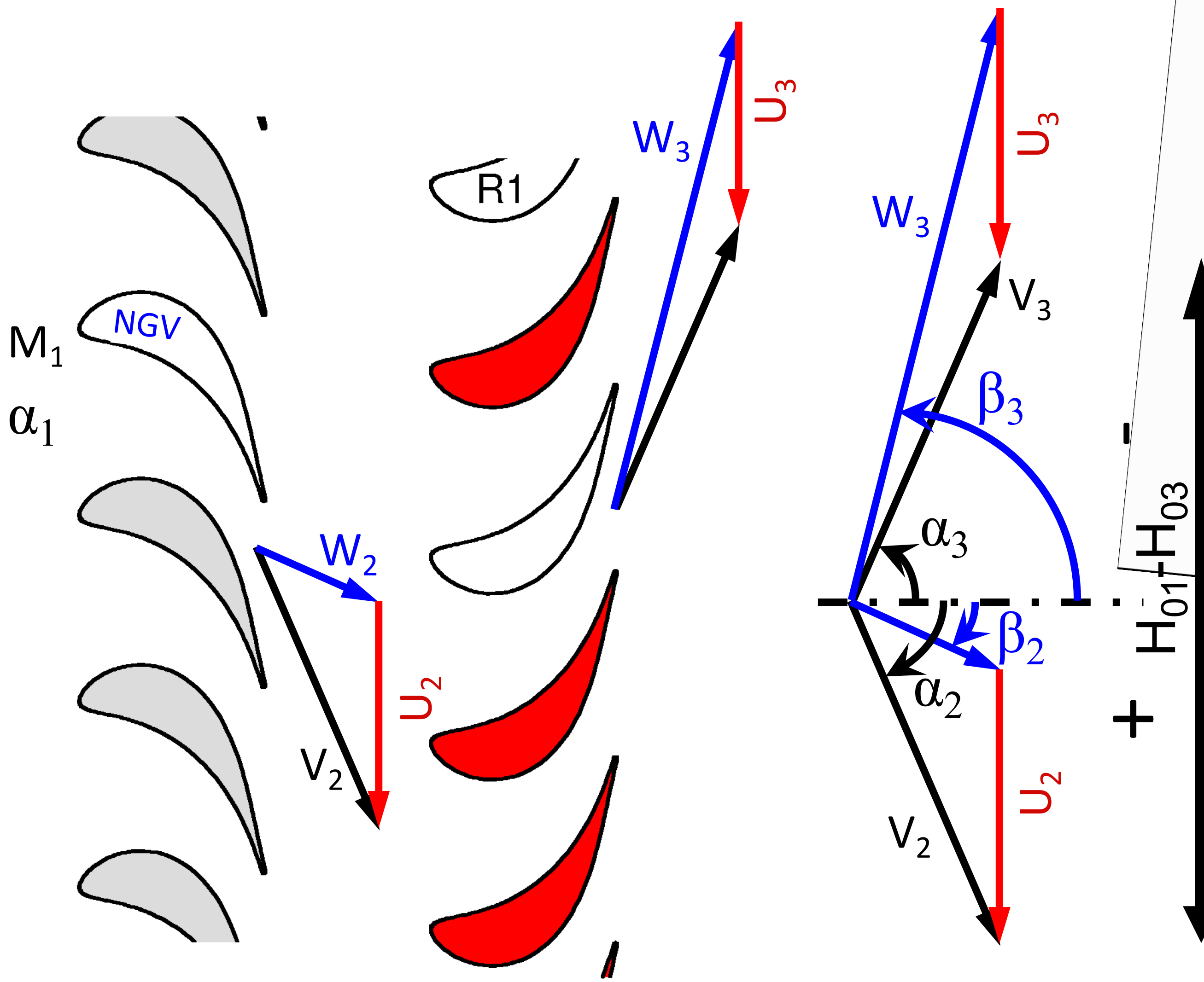

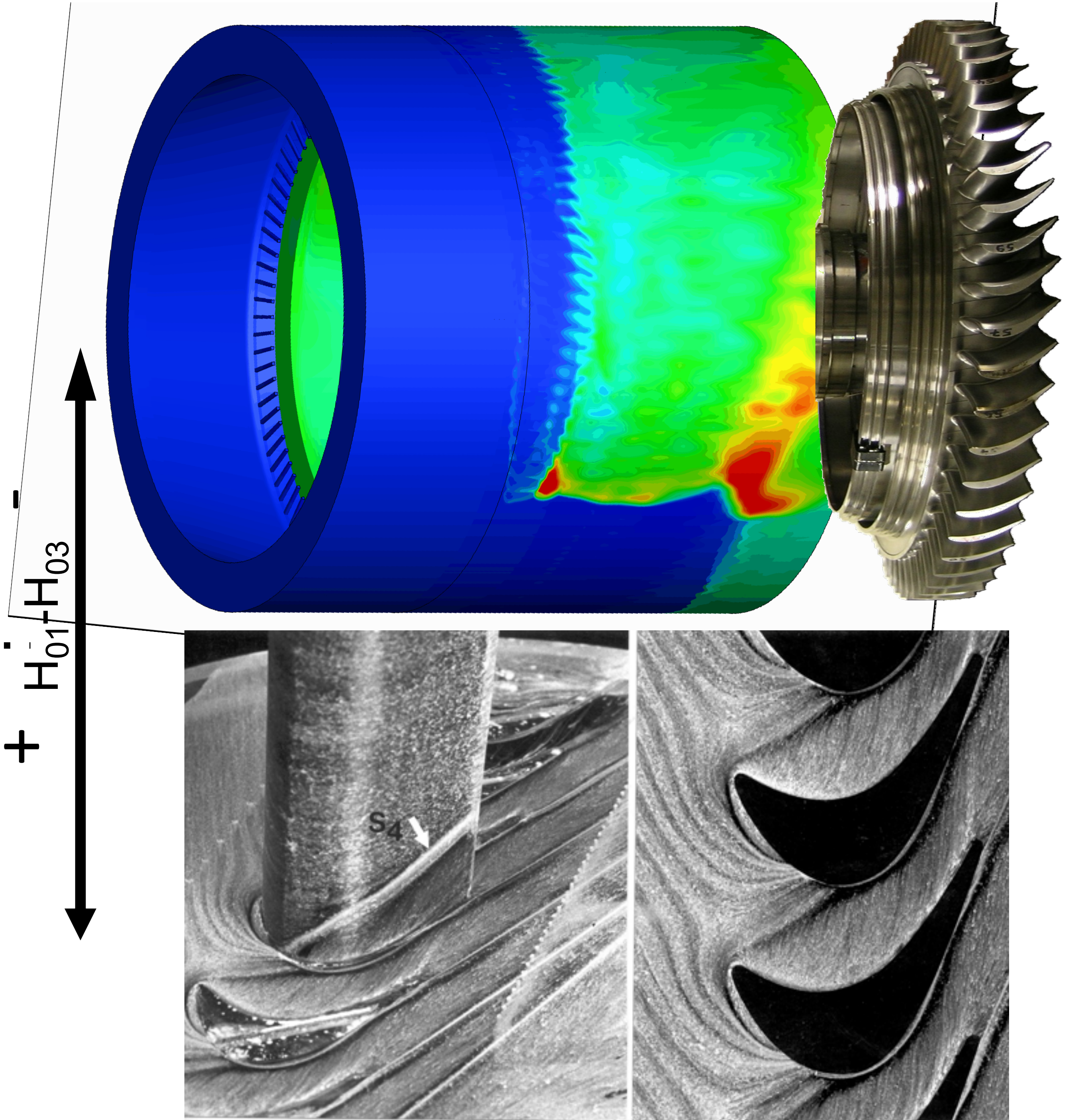

Turbomachinery II - ME533

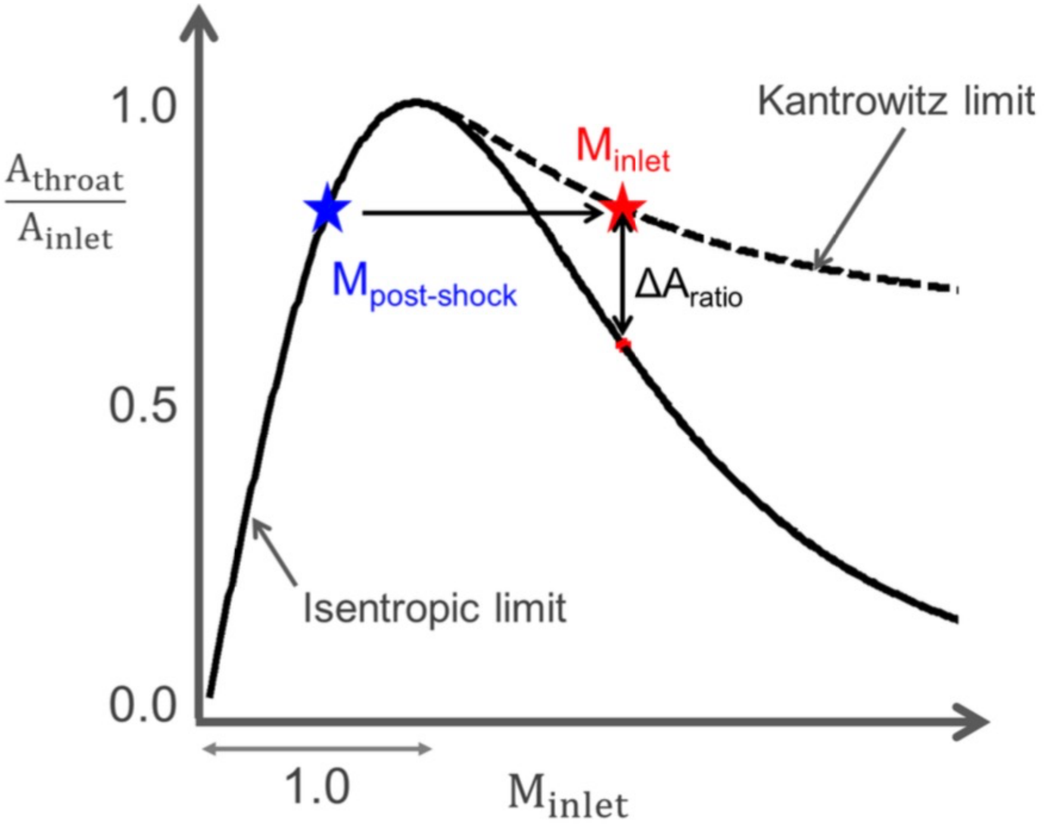

Sousa, Paniagua, 2015, http://doi.org/10.3390/e17085593

Sousa, Paniagua, Collado, 2022, https://doi.org/10.1016/j.cja.2022.04.003

M_{inlet}=0.2

M_{inlet}=2.0

OBJECTIVES

1. Improve turbine overall work extraction with a diffuser-turbine efficiency of 90%
2. Ensure adequate damping to the rotating blades
3. Air dilution lower than 200% & minimize heat fluxes

APPROACH

1. Optimization and assessment of an industrial turbine vane under pulsating high speed inlet flow
2. Design and assessment of an optimized axisymmetric diffuser under pulsating flow
3. Identify the scaling parameters that emulate the RDC outlet conditions to enable TRL2/TRL3 testing

TASKS

1. Project Management and planning (management plan & technology maturation plan)
2. Loss budgeting in a combustor & transition element & turbine 1st stator (nozzle guide vane - NGV)
3. Demonstration RDC-transition-NGV coupling towards work production
4. Scale exp. & comp. studies to F-class and aero-derivative RDE gas turbine integrated system

2: Loss budgeting in a combustor + diffuser + NGV (turbine 1st stator)

2.1 Identification of loss mechanisms for the combustor with turbine NGV (turbine 1st stator)

Initial work will focus on an existing combustor/diffuser/NGV geometry, followed by tests using optimized geometries (Task 3)
computational model validation, then predict the combustor losses of the larger-scale RDE combustor/diffuser/NGV
computational model will be used to minimize combustor losses in the final RDE-turbine geometry in Task 3

2.2 Quantification of the combustor/ turbine NGV (turbine 1st stator) performance metrics

single representative metric of combustor/diffuser/NGV performance will then be utilized
a new scheme leveraging the high-speed particle image velocimetry (PIV)
CARS & PIV data will be used to validate this approach

2.3 Uncertainty quantification of loss mechanisms by integrating high fidelity simulations with the experimental data

Large Eddy Simulations of the tested optical transparent RDC

Subtask 2.1 Identification of loss mechanisms for the combustor with NGV (turbine 1st stator)

identify loss mechanisms from diffuser/NGV integration through various high-speed non-intrusive diagnostics
provide benchmark validation data for high-fidelity simulations

Current tools

- High frequency wall-pressure measurements ($p_{stat.}$)
- MHz rate simultaneous orthogonal OH* chemiluminescence and OH-PLIF (χ^{OH^*} and χ^{OH})
- Exhaust chemiluminescence (χ^{OH^*})
- Femtosecond Laser Activation and Sensing of Hydroxyl radical (FLASH) velocimetry (v)
- Coherent vortex-velocimetry (v)

Under development

- MHz rate high speed optical parametric oscillator(OPO)
  - OH-PLIF measurements
  - FLASH
  - Coherent vortex-velocimetry
- 100 kHz – 1MHz ps-CARS system for
  - Exhaust temperature measurements
- 1 kHz hybrid CARS system (fs/ps CARS)
  - Temperature inside the RDC annulus

No NGV installed

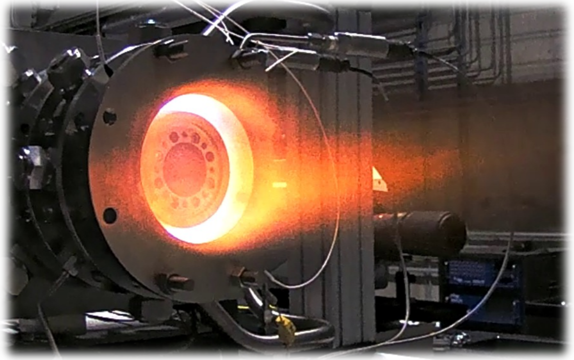

- *Azimuthal Reflected Shock Combustion (ARSC) –* ***P_{tot} Loss***
- *Exhaust velocity variations*
- *Effect of stator blades on combustor performance*
- *Validation data and CFD comparison*

NGV installed

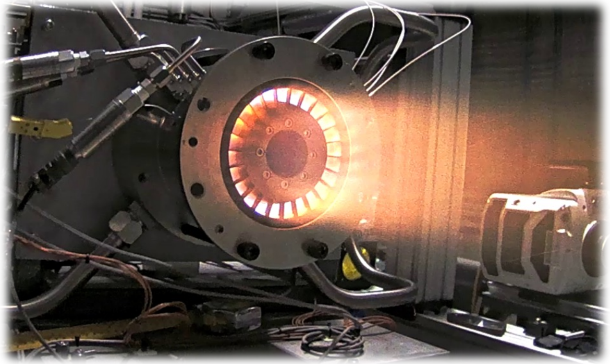

Liu Z., Paniagua G., 2018, https://doi.org/10.1115/1.4037640

Athmanathan, Fisher, Ayers, Glez Cuadrado, Andreoli, Braun, Meyer, Paniagua, Fugger, Roy, 2019, https://doi.org/10.2514/6.2019-4041

Subtask 2.1 Identification of loss mechanisms for the combustor with NGV (turbine 1st stator)

- **3-D detonation structure** captured using simultaneous MHz orthogonal OH-PLIF and OH* chemiluminescence[1]
  - OH* Chem – captures flame front in axial-azimuthal **(x – θ)** direction (loses radial depth information)
  - OH PLIF– captures flame front in radial-axial **(x – r)** direction (loses azimuthal information)
- Hydroxyl radical (OH) is an important species because it provides reaction zone and combustion products visualization
- New in-house custom laser source built to uniquely enable MHz speeds for in-situ spatially resolved RDE diagnostics

Simultaneous orthogonal views of OH and OH*

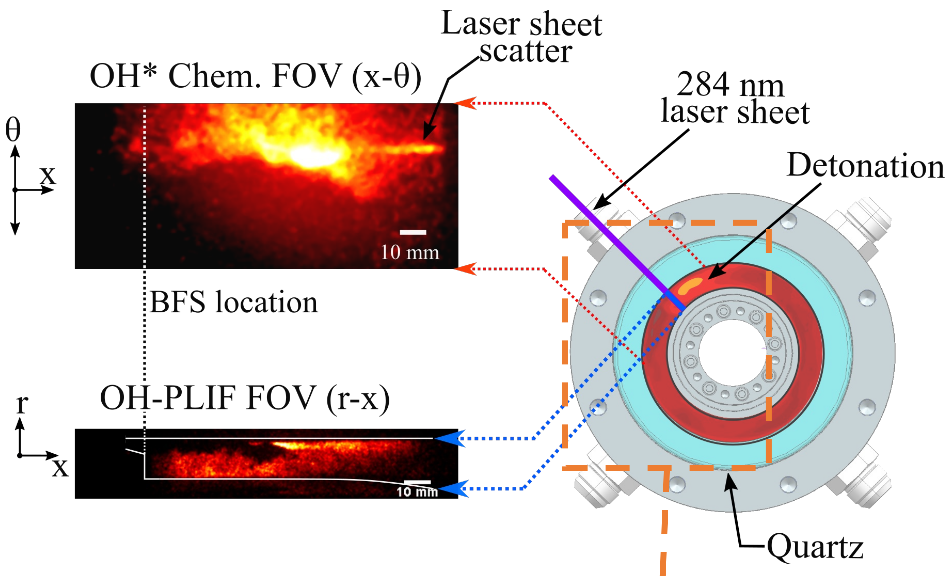

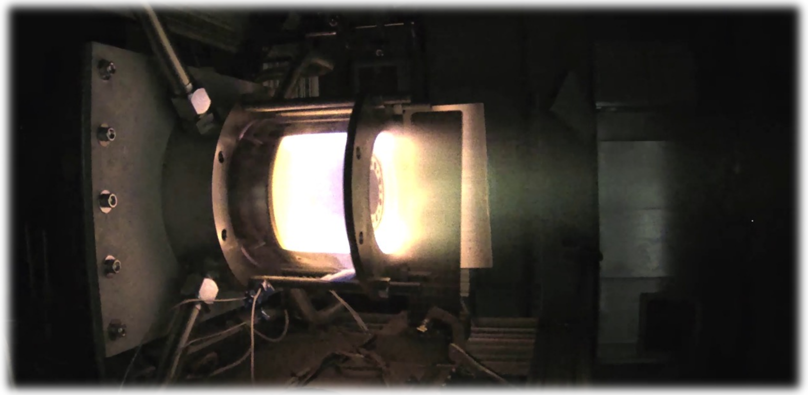

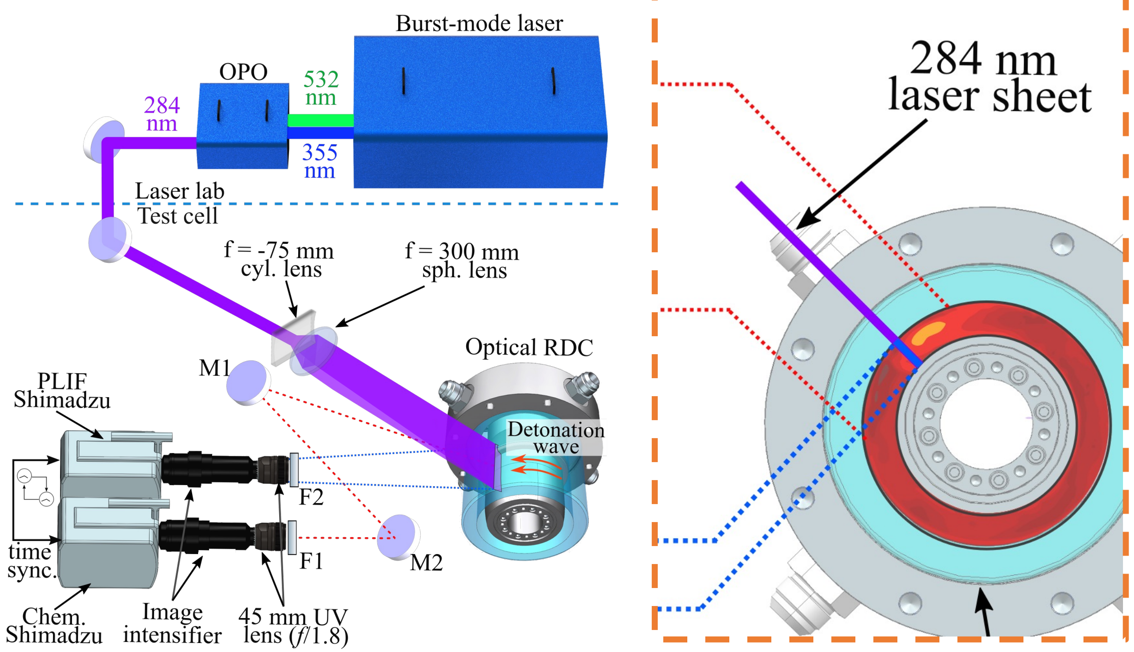

Subtask 2.1 Identification of loss mechanisms for the combustor with NGV (turbine 1st stator)

***3-D detonation structure** captured using simultaneous MHz orthogonal OH-PLIF and OH* chemiluminescence[1]*

MHz video sequence [1]

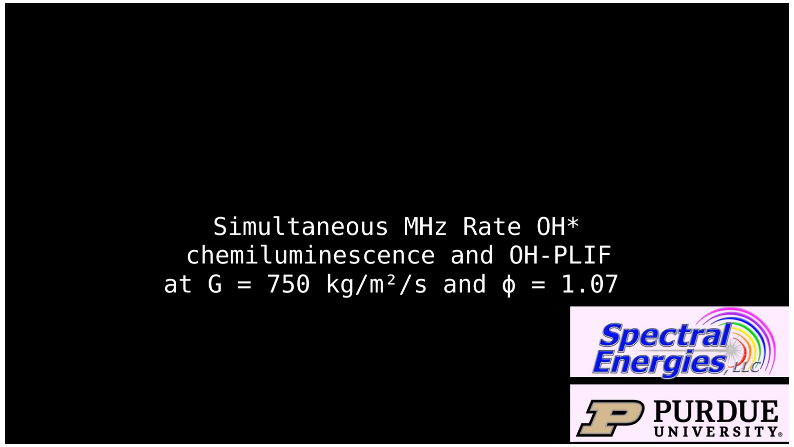

Zone Bifurcation

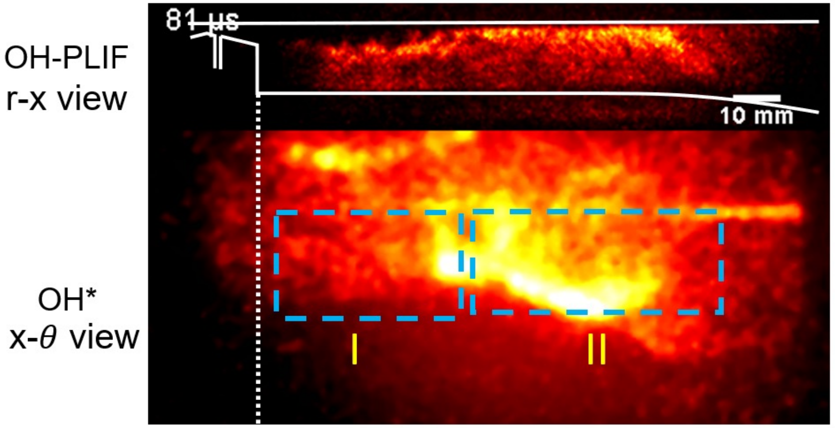

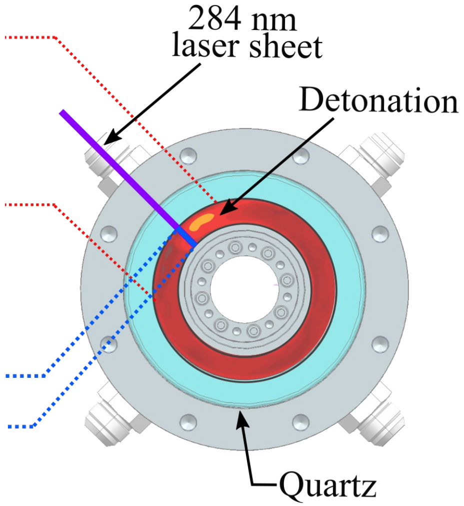

OH-PLIF | Wave Pos. | OH* Chem.

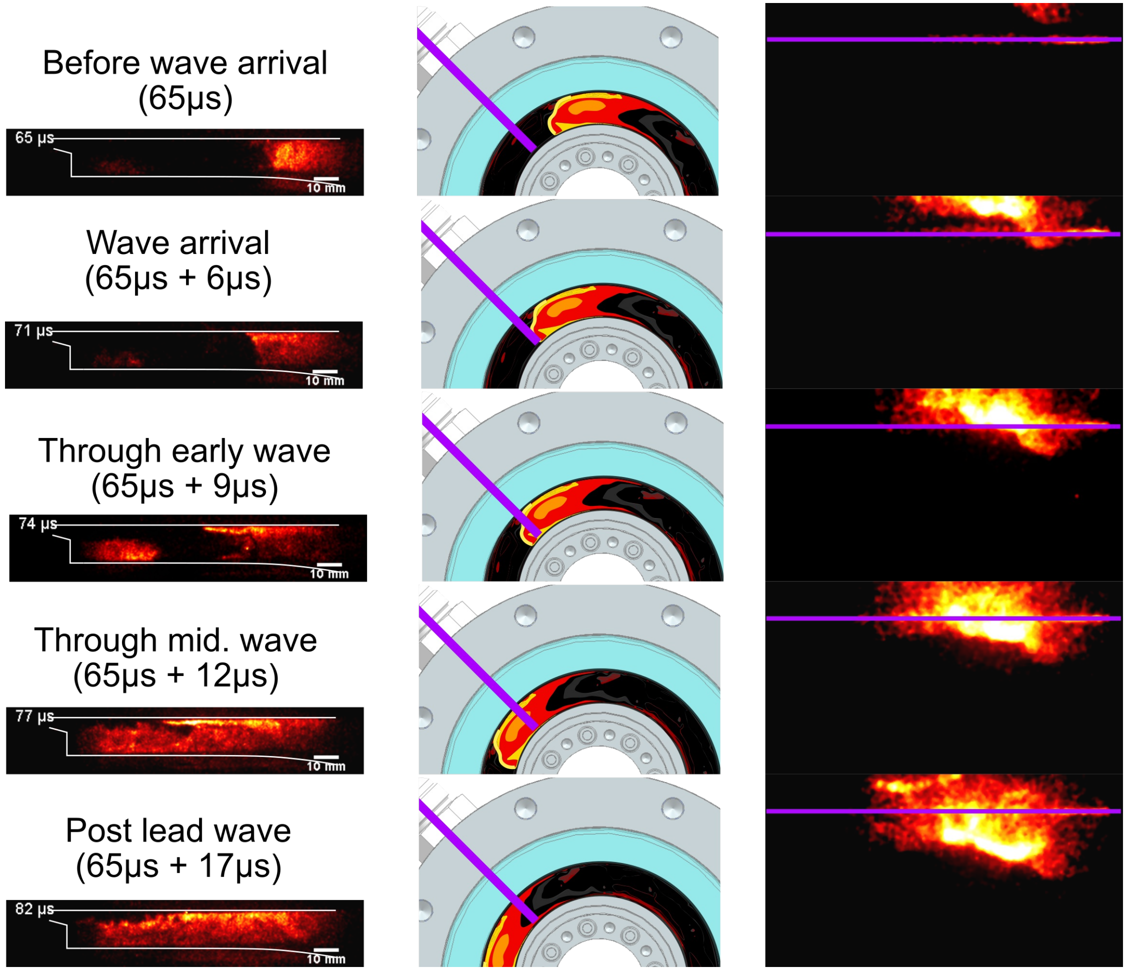

Athmanathan,, Braun, Ayers, Fugger, Webb, Slipchenko, Paniagua, Roy, Meyer. Combustion and Flame 240 (2022)

Subtask 2.1 Identification of loss mechanisms for the combustor with NGV (turbine 1st stator)

Key Result

- The ARSC zone is detonative in nature
- For shock induced/flow induced detonation two characteristics (Pratt, 1991 JPP)
- Shock formed by external source (leading detonation)

Experimental Evidence	Numerical Evidence
(a) Thin heat release (< 2 mm)	(a) Shock flame coupled (< 2 mm)
(b) Chemiluminescence intensity of ARSC comparable to Zone I	(b) Product gas acceleration
	(c) T_{total} and P_{total} ⇧

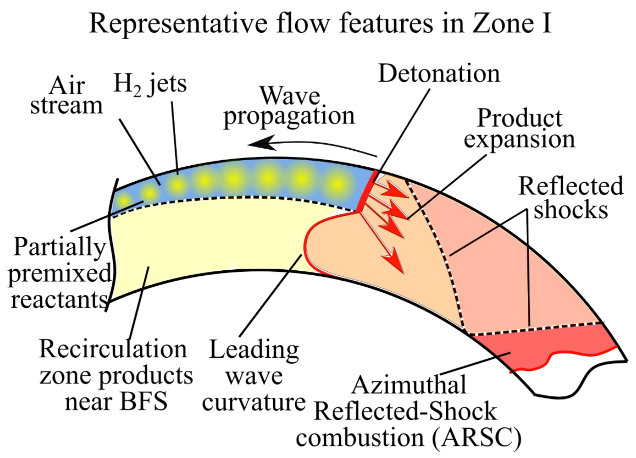

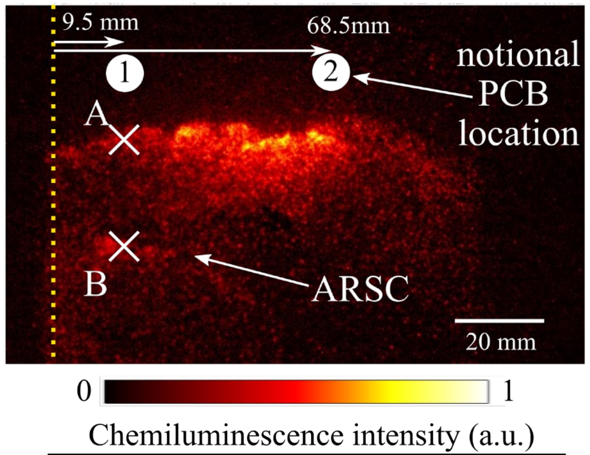

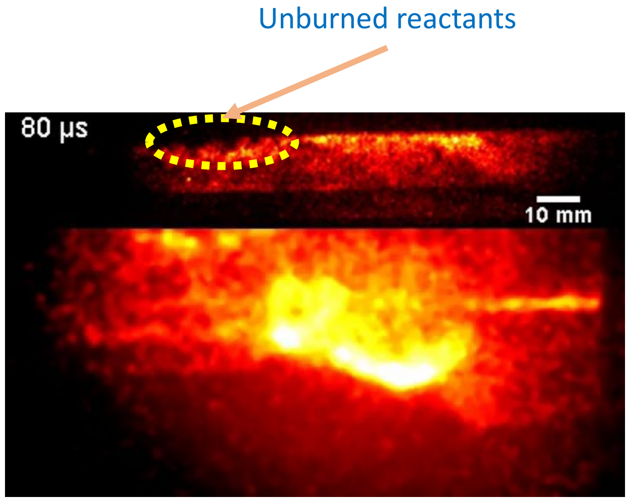

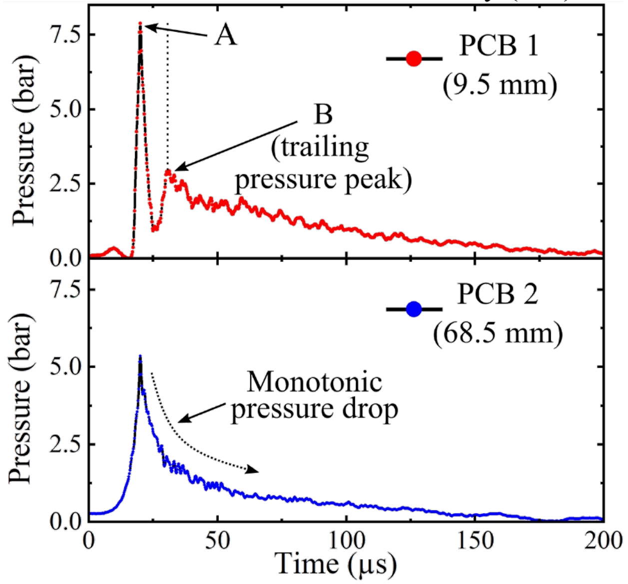

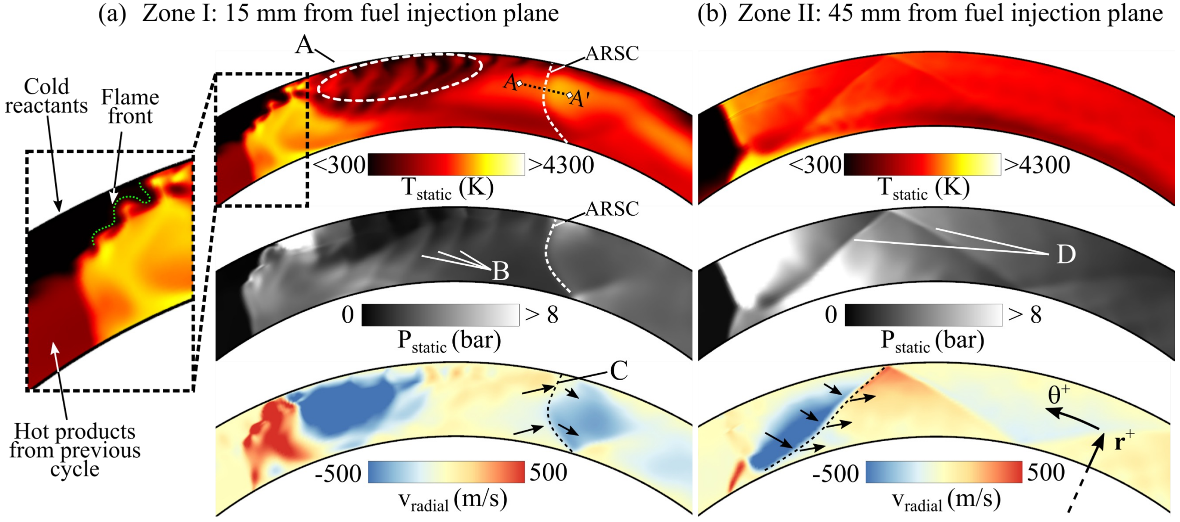

[1] Athmanathan, Venkat, James Braun, Zachary M. Ayers, Christopher A. Fugger, Austin M. Webb, Mikhail N. Slipchenko, Guillermo Paniagua, Sukesh Roy, and Terrence R. Meyer. "On the effects of reactant stratification and wall curvature in non-premixed rotating detonation combustors." *Combustion and Flame* 240 (2022): 112013.

Subtask 2.1 Identification of loss mechanisms for the combustor with NGV (turbine 1st stator)

- **Operating conditions**
  - m = 1 lbm/s with $\Phi_{global} = 1.0 \pm 0.05$
- **CHV** - Identify coherent structures and track the 'luminosity' to obtain V
- **FLASH** – Tracks OH cluster created by fs-laser
- MHz rate measurements, wave position tracked during measurement

- Velocities as high as 1000 m/s observed in the exhaust
- Flow angles (θ) as high as 90° (purely azimuthal velocity)
  - Flow can be 'purely' azimuthal with low axial velocities.
  - **Methods such as EAP, which ignore V_θ may not capture the full P_{gain}**
- Results compared with CFD and show close match.

Experimental Setup

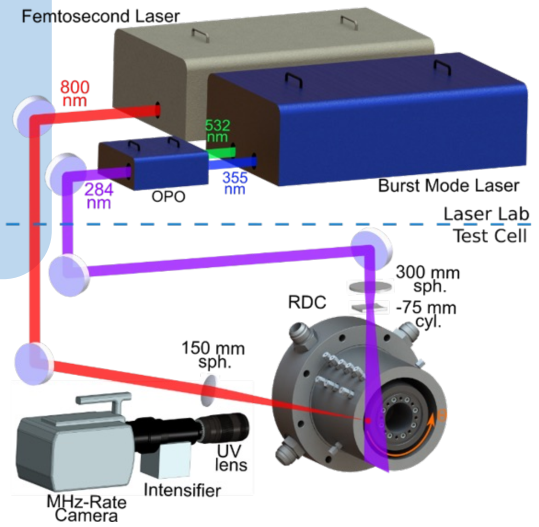

Field of View (Exhaust)

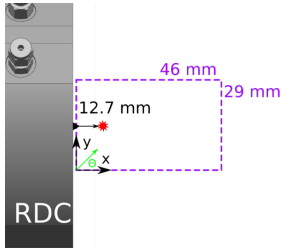

FLASH Plasma tracking (1 MHz)

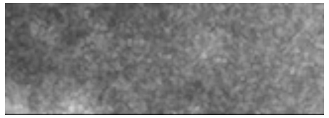

Net velocity (m/s)

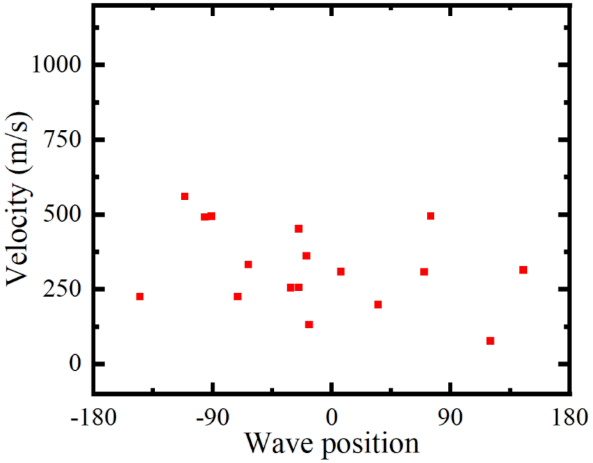

Flow angle(θ)

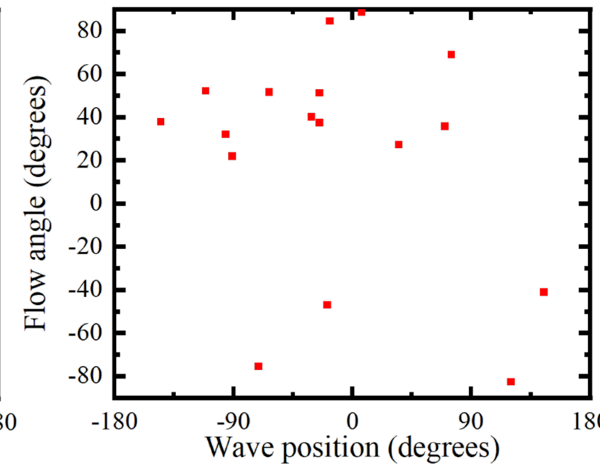

Axial velocity (m/s)

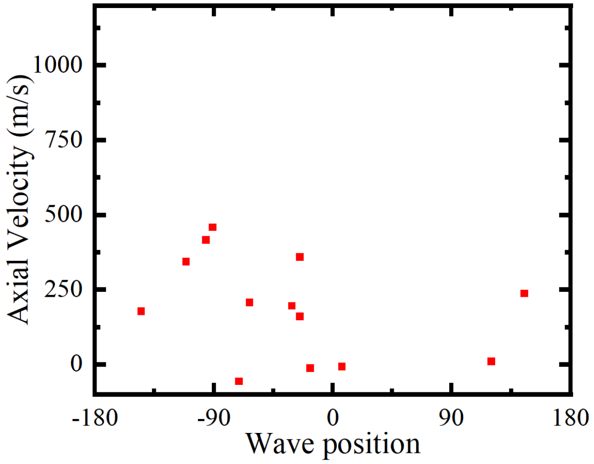

CHV Flash Comparison

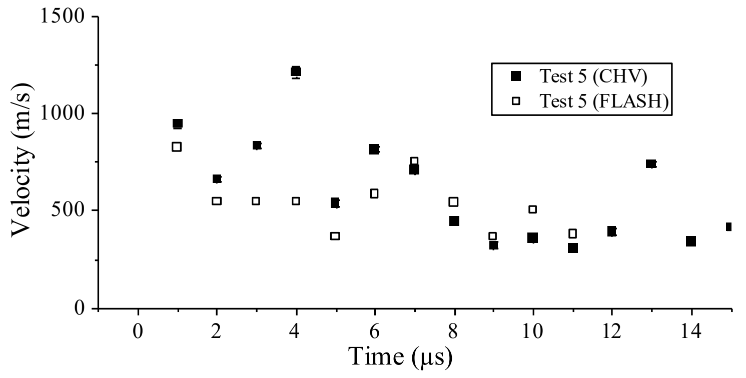

Subtask 2.1 Identification of loss mechanisms for the combustor with NGV (turbine 1st stator)

NGV effect on RDC performance

- **Operating conditions**
  - m = 0.5 to 2 lbm/s with $\Phi_{global} = 1.0 \pm 0.05$
- **Wave Frequency (<5%)**
  - **No influence of NGV on wave frequency**
- **Pressure profile**
  - Nearfield: Profile remained consistent with a 'dual-wave structure' – indicative of ARSC combustion
  - Farfield: Profile reduced in width – indicating an increase in detonation strength due
    - Common trend for all air mass flow rates
    - 16 us FWHM in the far-field without stator
    - 5.40 us FWHM in the near-field with stator, 66% decrease in FWHM

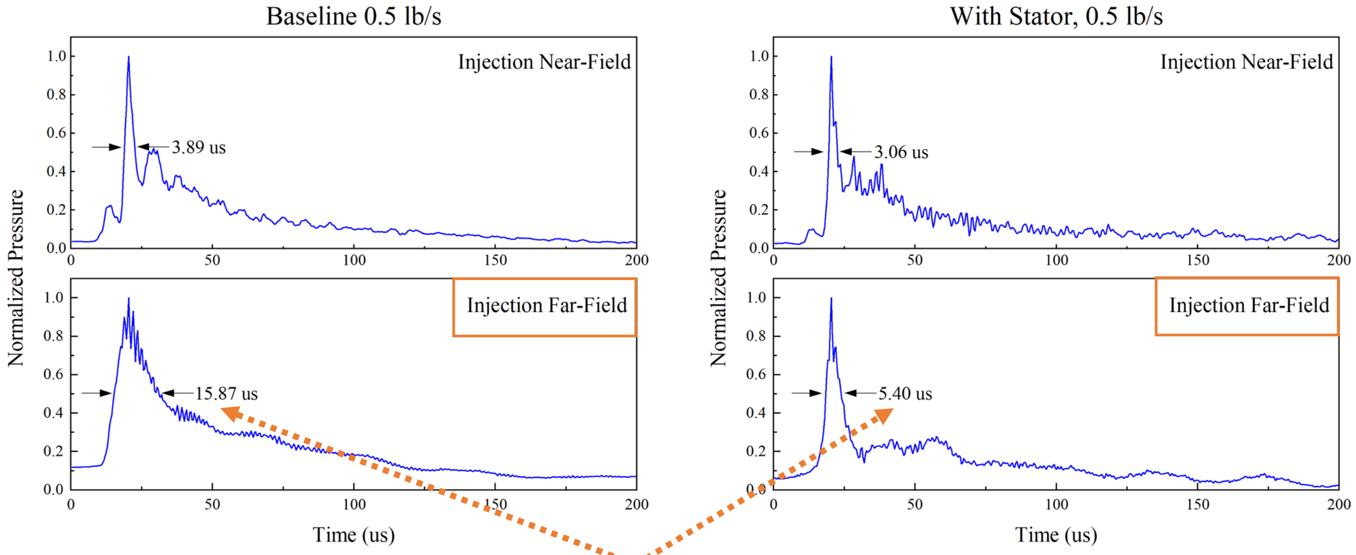

Similar trend for all flow rates

RDC operation with NGV

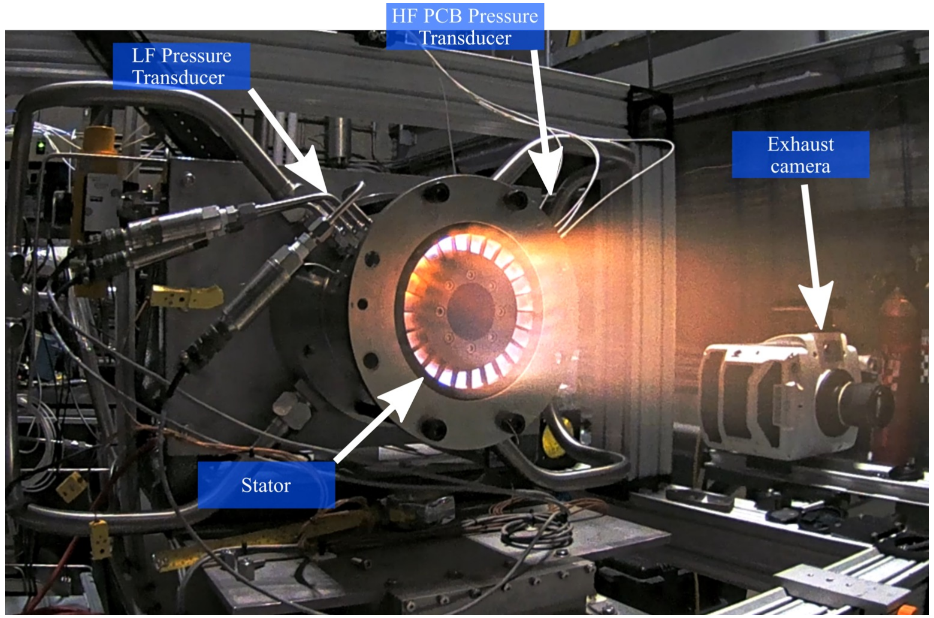

Instrumentation

- High frequency flush mounted PCBs installed on THOR hardware
- Injection nearfield (1) and far-field (2) PTs were analyzed

Flush mounted PCB

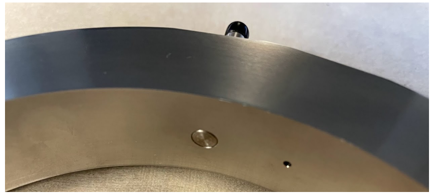

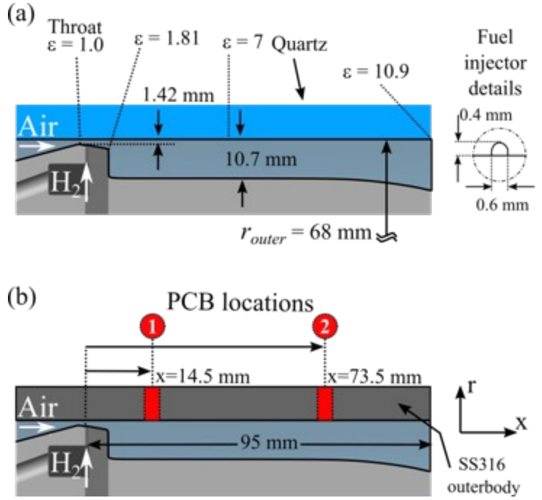

Subtask 2.1 Identification of loss mechanisms for the combustor with NGV (turbine 1st stator)

NGV effect

- **Operating conditions**
  - m = 0.5 to 2 lbm/s with $\Phi_{global} = 1.0 \pm 0.05$
- **Wave Frequency (<5%)**
  - **No influence of NGV on wave frequency**
- **Pressure profile**
  - Nearfield: ‘dual-wave structure’ – indicative of ARSC
  - Farfield: Profile reduced in width
- **Other invariant parameters (< 5%)**
  - Gross base-pressure uncorrected thrust
  - Mean chamber pressure

RDC operation with NGV

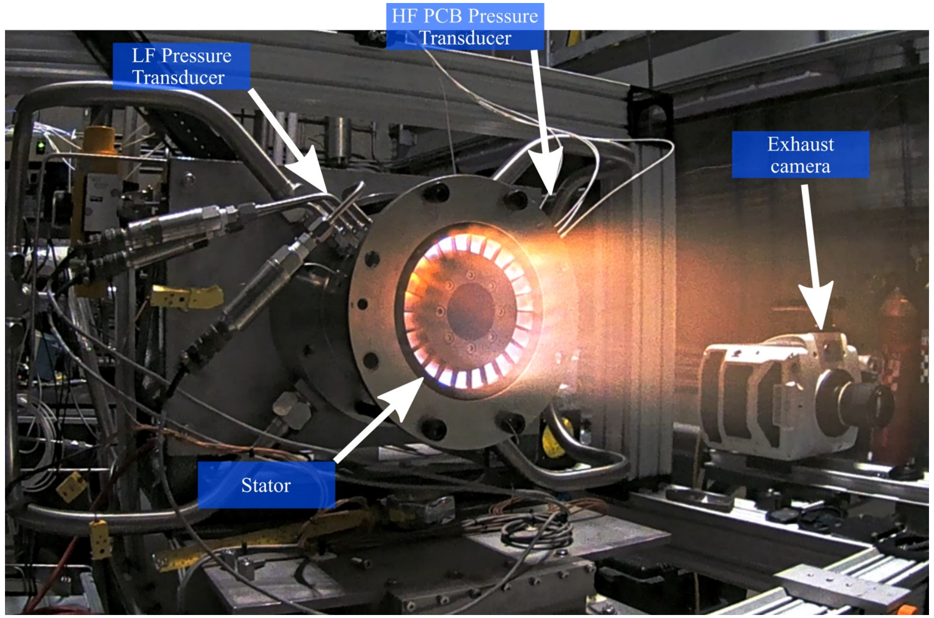

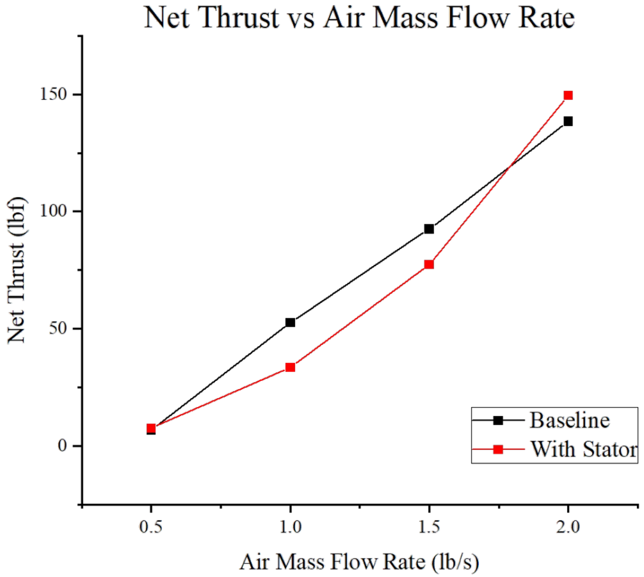

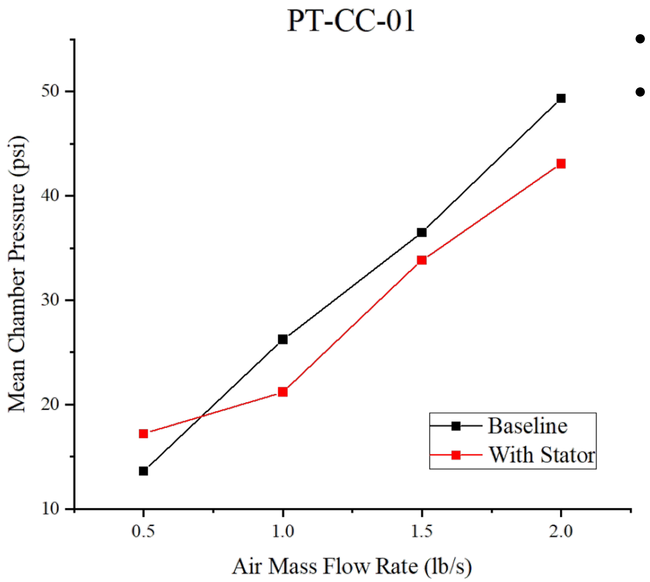

Instrumentation

- High frequency flush mounted PCBs installed on THOR hardware
- Injection nearfield (1) and far-field (2) PTs were analyzed

Flush mounted PCB

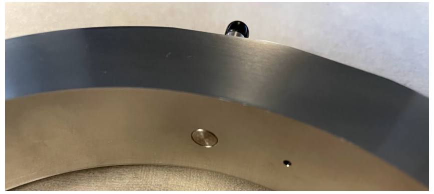

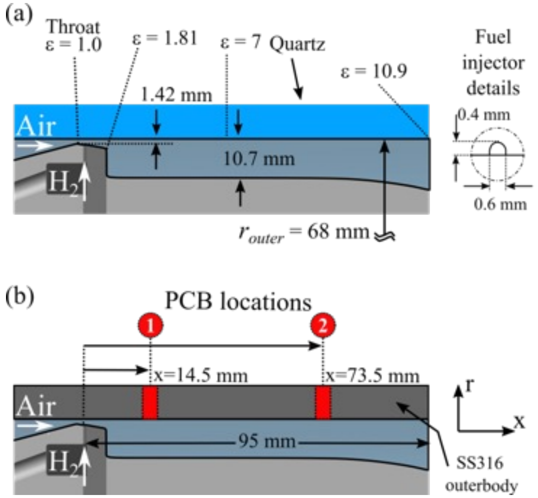

Subtask 2.3 Uncertainty quantification of loss mechanisms

High-fidelity LES of THOR RDC

- A wall-modeled large-eddy simulation (WMLES) was developed to capture the detonation wave dynamics in the THOR RDC
- The LES modeling framework leverages adaptive mesh refinement (AMR), hydrogen/air detailed chemistry (9-sp, 21-rxns), and dynamic structure subgrid turbulence model
- One operating condition corresponding to fuel and air mass flow rates of 0.035 kg/s and 1.2 kg/s (global equivalence ratio = 1), respectively, was simulated
- A non-reacting flow simulation was first run until steady state; the steady-state solution was then used to initialize the reacting flow simulation; the RDC was ignited using a predetonator tube
- Similar to experiment, a strong detonation wave was observed along with a trailing wave at quasi-steady state
- Quantitative validation of LES against experimental data and comparison with URANS simulations are currently underway
- Post-processing tools are being developed to extract the relevant quantities of interest from the LES that are associated with losses within the RDC, and RDC aerodynamic/thermal performance

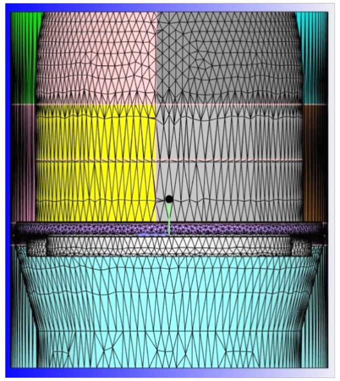

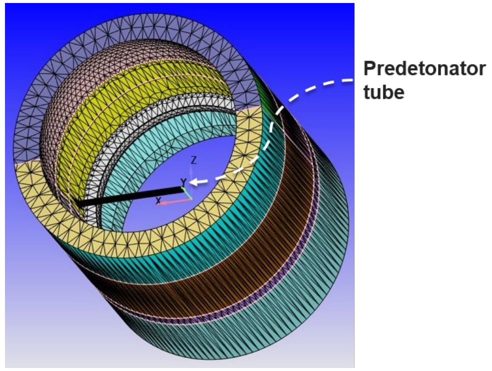

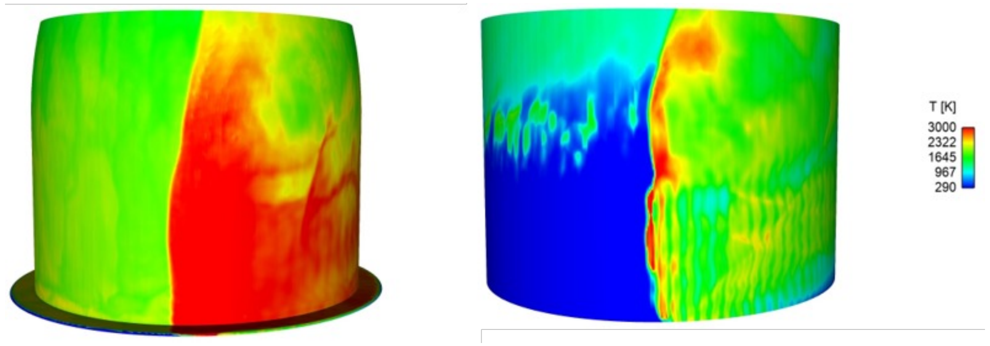

RDC Inner Wall

RDC Outer Wall

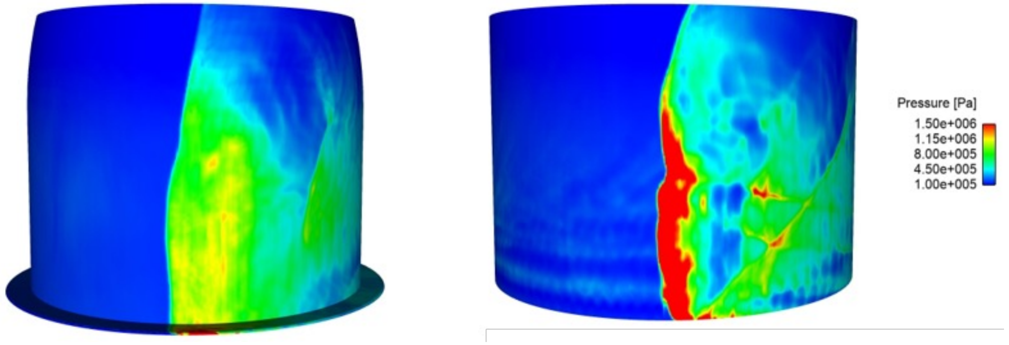

Subtask 2.3 Uncertainty quantification of loss mechanisms

High-fidelity Large-eddy Simulation (LES) of THOR H_2/air RDC

Detonation wave structure

- Single detonation wave behavior is observed
- A trailing azimuthal reflected shock combustion (ARSC) wave is observed behind the leading detonation wave

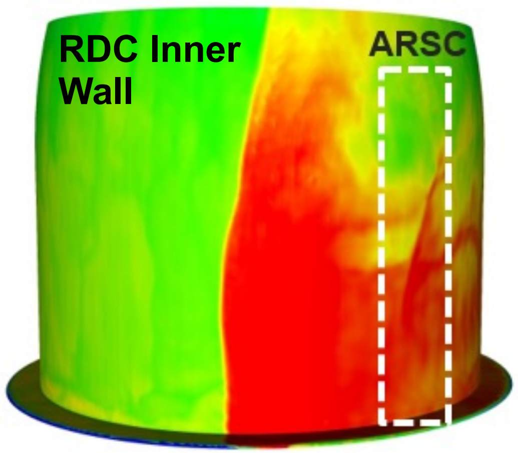

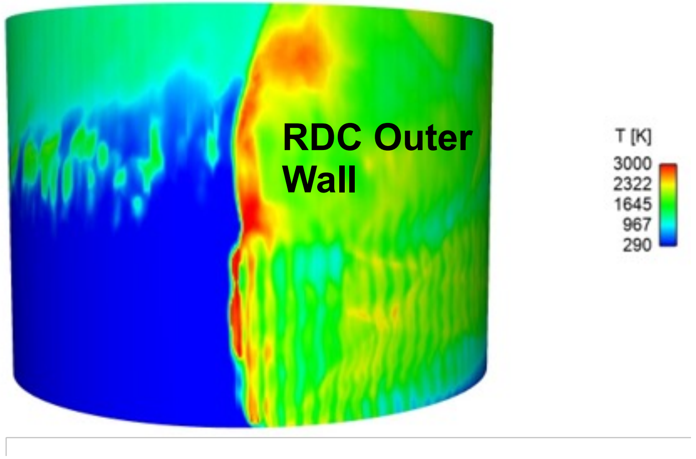

- LES depicts similar qualitative wave structure as experiments
- The high-fidelity LES results were employed to benchmark the Purdue URANS simulations
- Further analysis of LES data is currently underway to investigate the details of loss mechanisms within the RDC

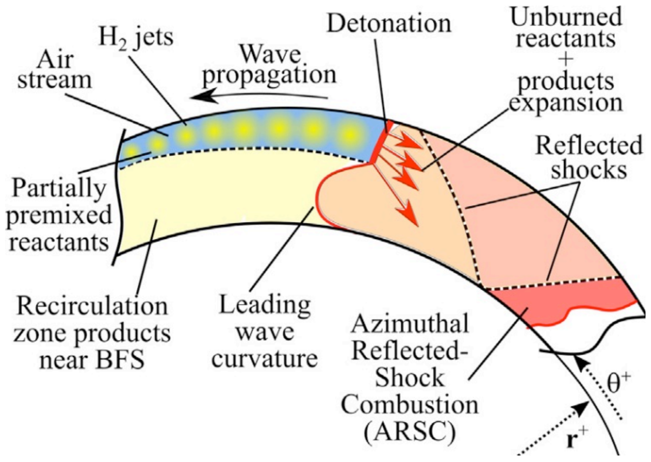

Athmanathan et al., CNF 2022

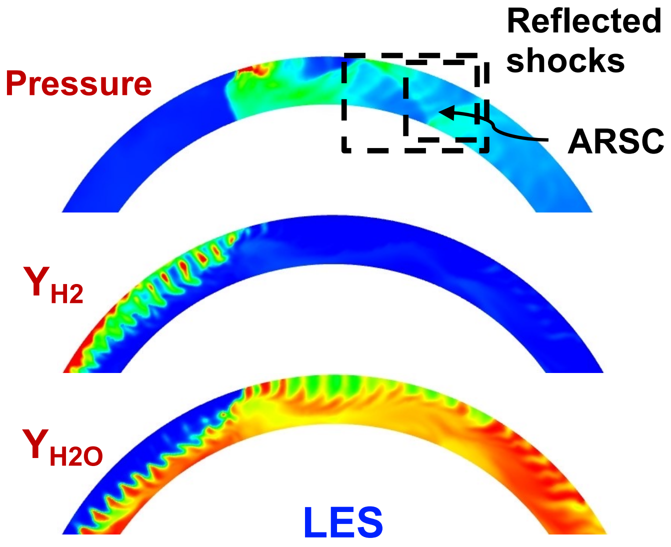

3: Demonstration RDC - transition element – NGV (1st stator) towards work production

3.1 Overall transition element optimization

definition of the inlet conditions

Multi-objective optimization using genetic algorithms of the 16 param that defines the geometry

full unsteady simulations with 3 different combustor wave modes will be used to assess the diffuser performance

3.2 Computational multi-objective optimization of the NGV (turbine 1st stator)

multi-objective differential evolutionary optimization strategy

objective 1 - Abate tonal noise & harmful structural vibrations

objective 2– Increase efficiency

optimization run first on the vane alone, then performance assessed with a full turbine stage unsteady simulation

3.3 Experimental demonstration of the transition element + NGV @warm conditions (600K)

aerothermal testing in the Big Rig of Aerothermal Stationary Turbine Analysis

3.4 Experimental demonstration of the optimal combustor + transition + NGV @hot conditions (1,700K)

aerothermal testing in RDC+M250 (RR engine)

Subtask 3.1 Overall transition element optimization – overall strategy

A. the combustor

feed boundary conditions →

3D reactive unsteady RANS

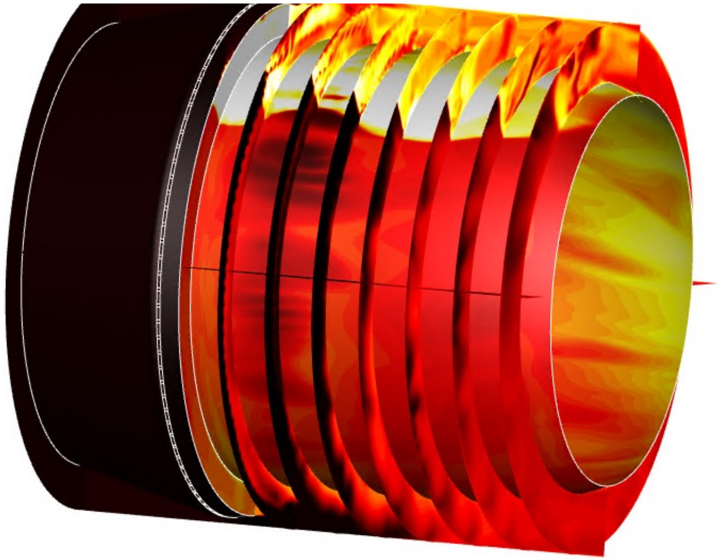

Objectives

-outlet conditions
-selection of operating point according to the pressure ratio

$$\textit{Pressure ratio} = \frac{p_{total,inlet}}{p_{static,exit}}$$

-pressure losses & enthalpy
-selection of relevant data for experimental validation

B. the combustor-diffuser

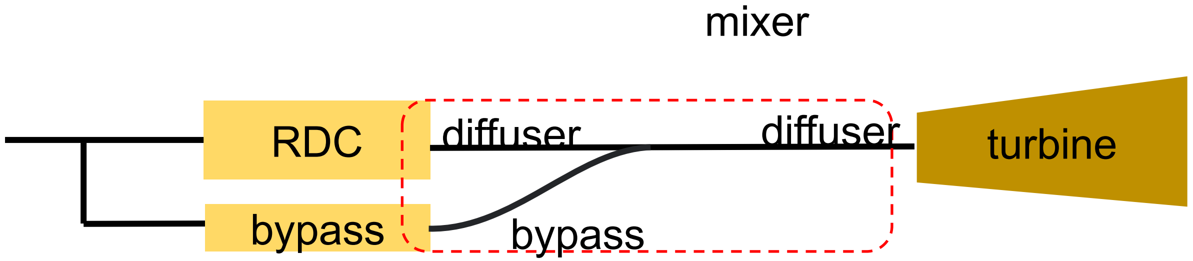

STEP 1: transition element: 0D/ 2D/3D RANS of the diffuser without bypass

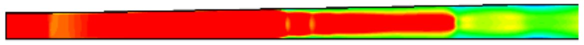

-diffuse the flow down to required Mach number
-quantify fluctuations

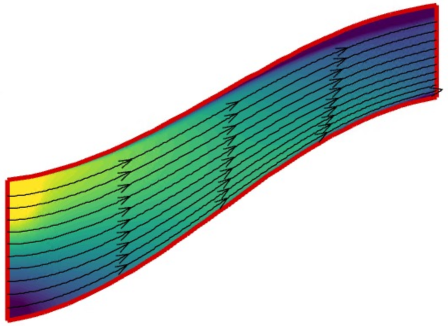

STEP 2: optimization of the bypass

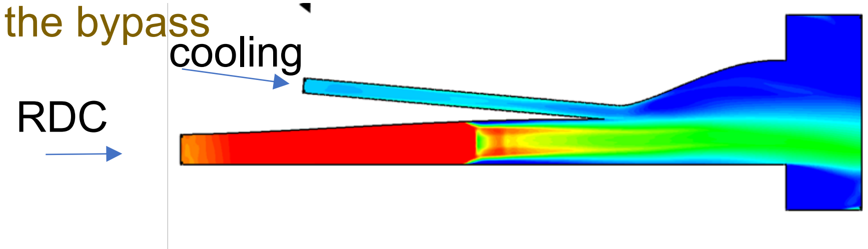

Subtask 3.1 Overall transition element optimization – RDC outlet conditions

-3D URANS (CFD++)
-1 step reaction mechanism
-structured mesh with Boundary layer
-pressure ratio of 2

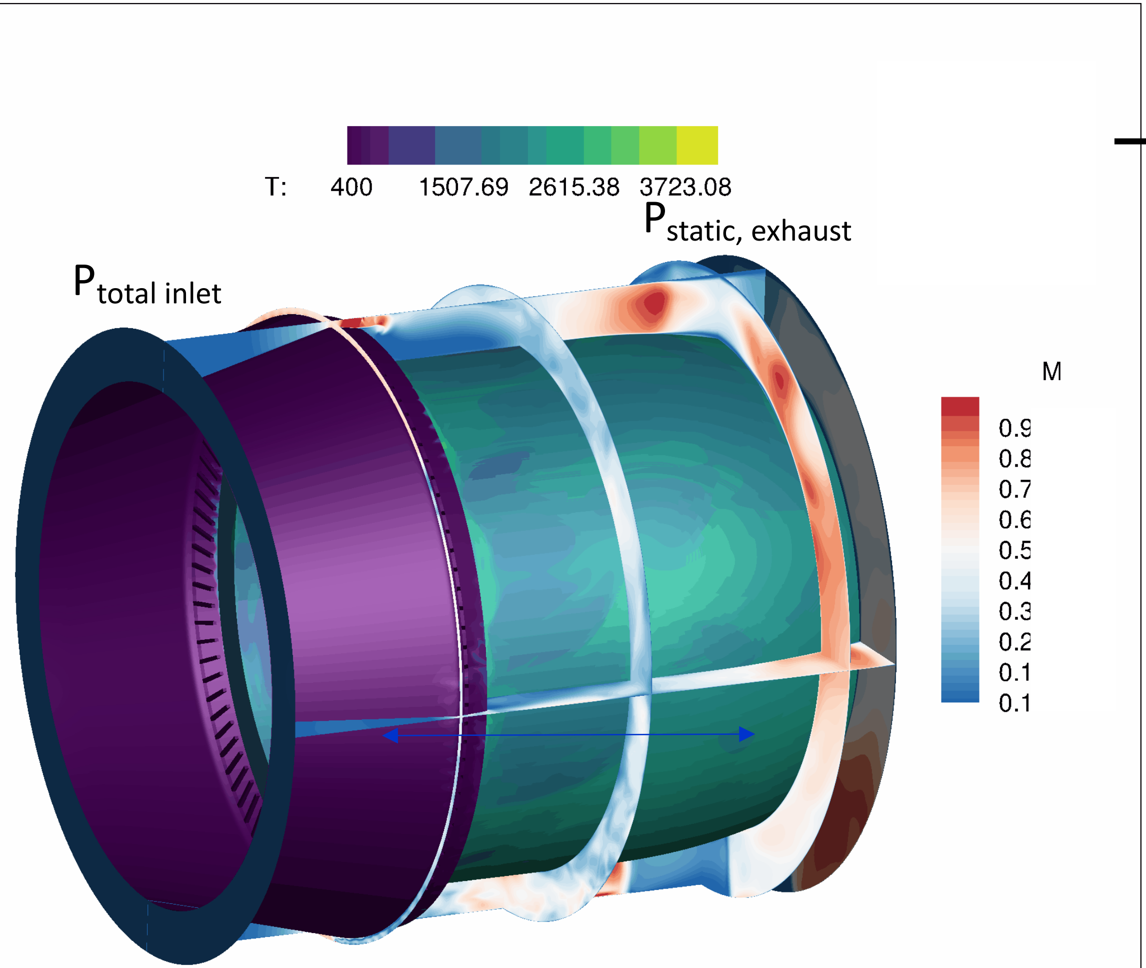

Pressure ratio($P_{total\ inlet}/P_{static,\ exhaust}$) *= 2*

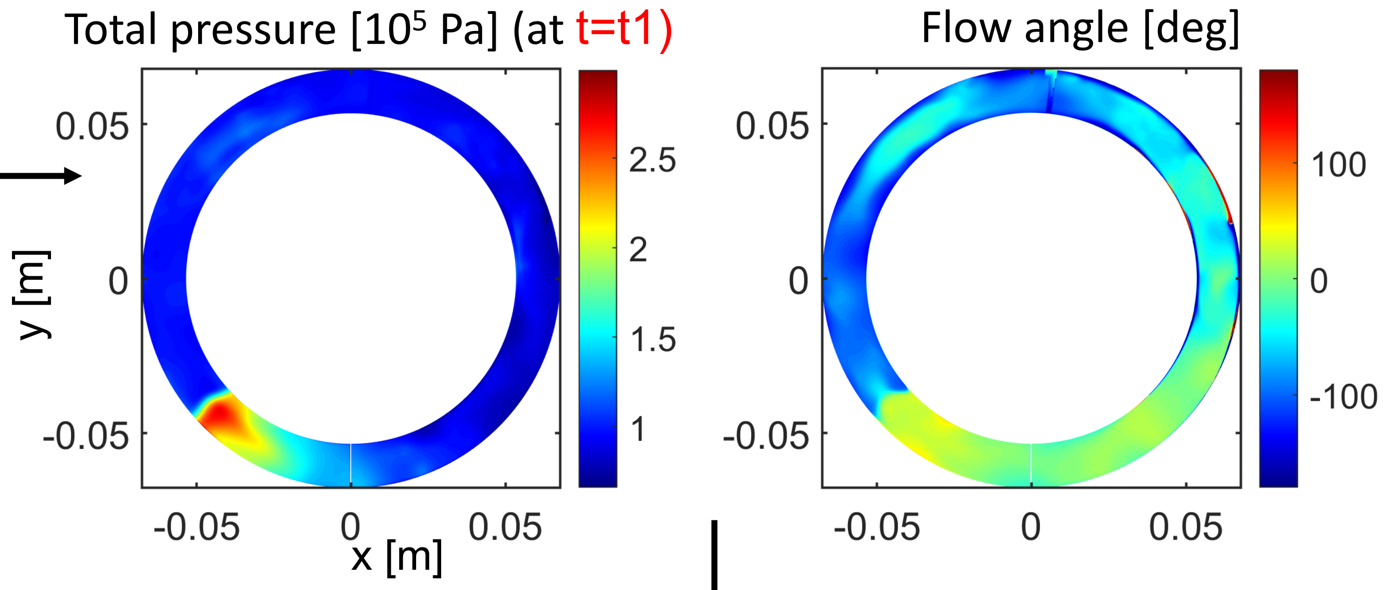

Radially mass flow averaged total pressure at 1 time instant

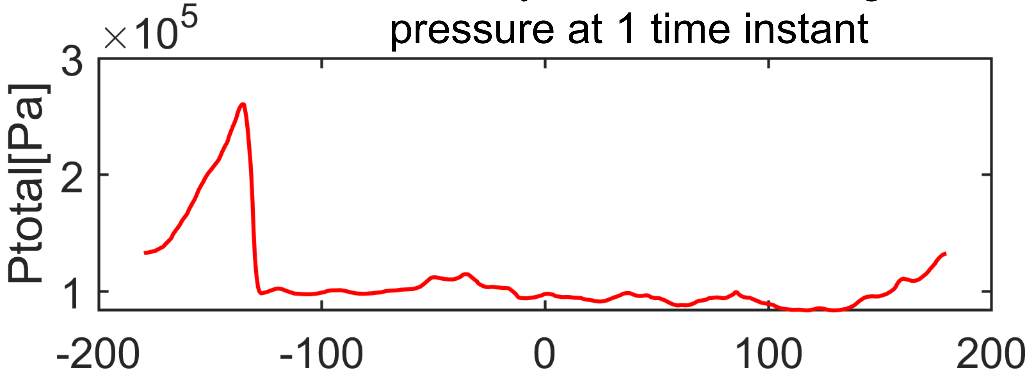

Subtask 3.1 Overall transition element optimization – RDC outlet conditions

Pressure ratio of 1.4

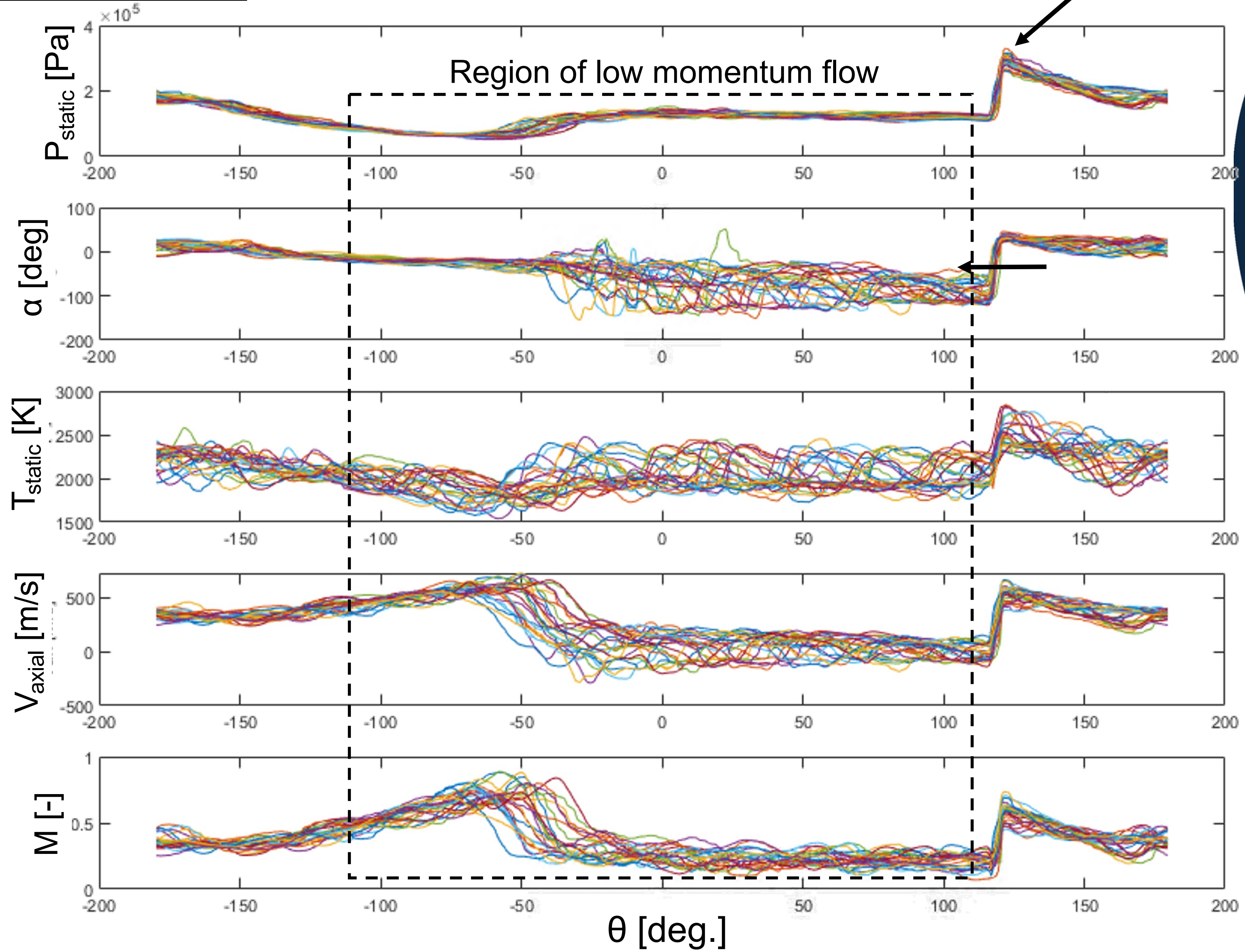

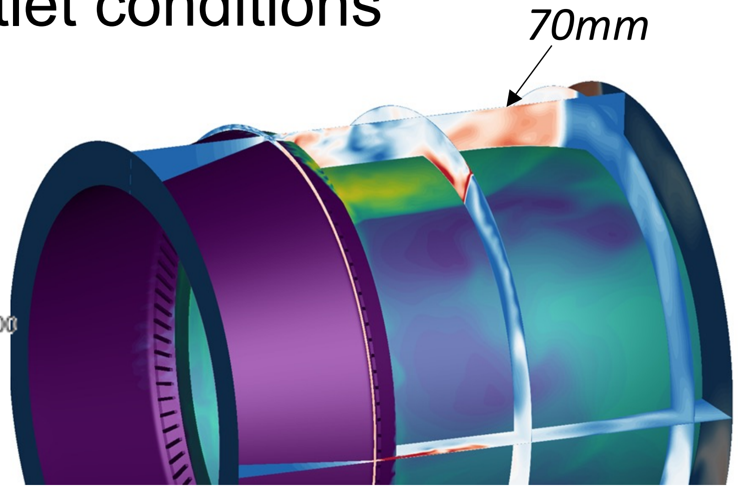

Pressure ratio of 1.4

**Different colors = different time steps*

Subtask 3.1 Overall transition element optimization

$$M_{mass\ flow\ av.} = \int \frac{\int M.u_{axial} \cdot \rho\, dA}{\int u_{axial} \cdot \rho\, dA} dt/\Delta t$$

Exit Mach number versus pressure ratio

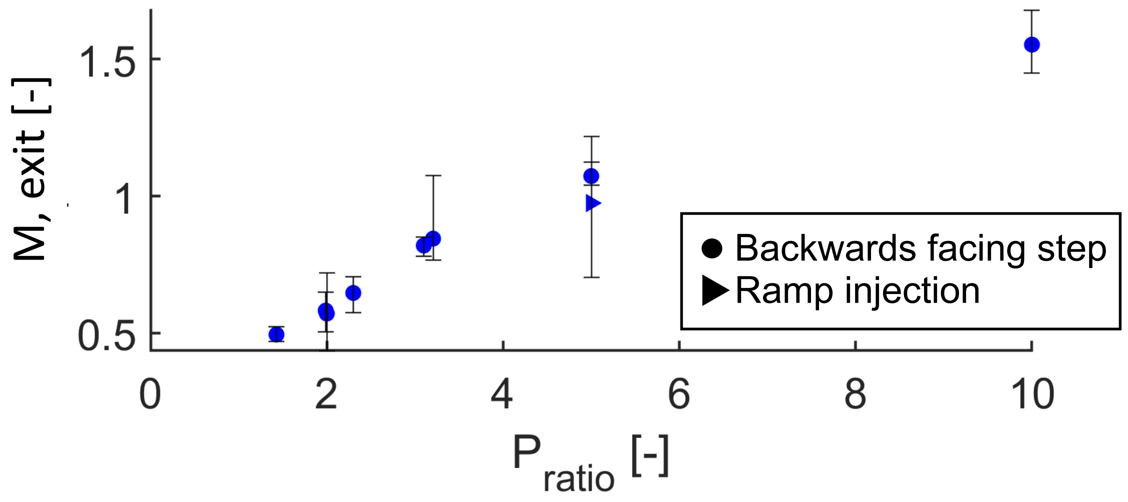

Backwards-facing step

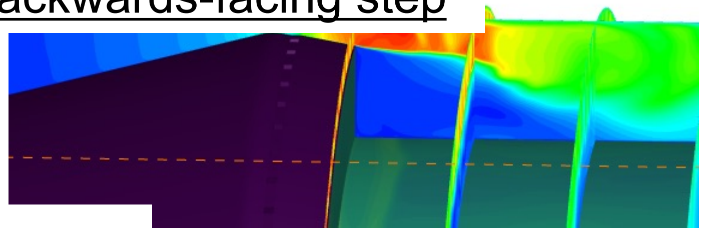

ramp

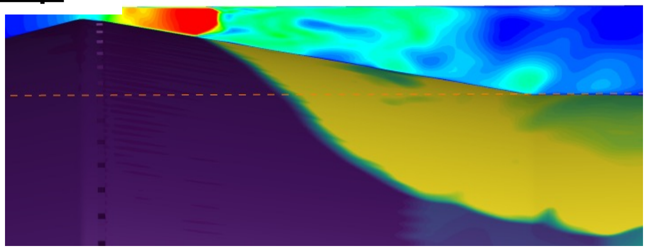

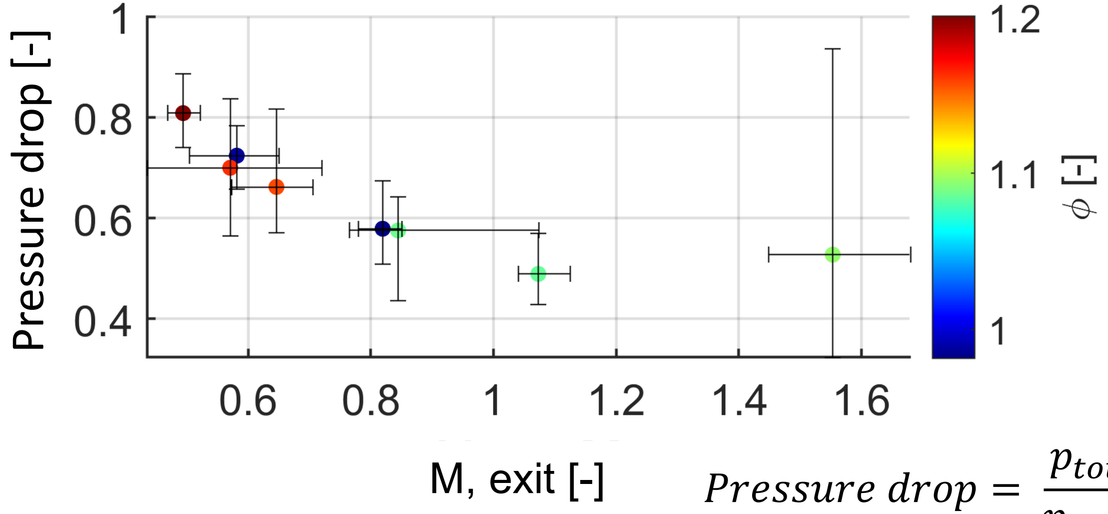

$$Pressure\ drop = \frac{p_{total,exit}}{p_{total,inlet}}$$

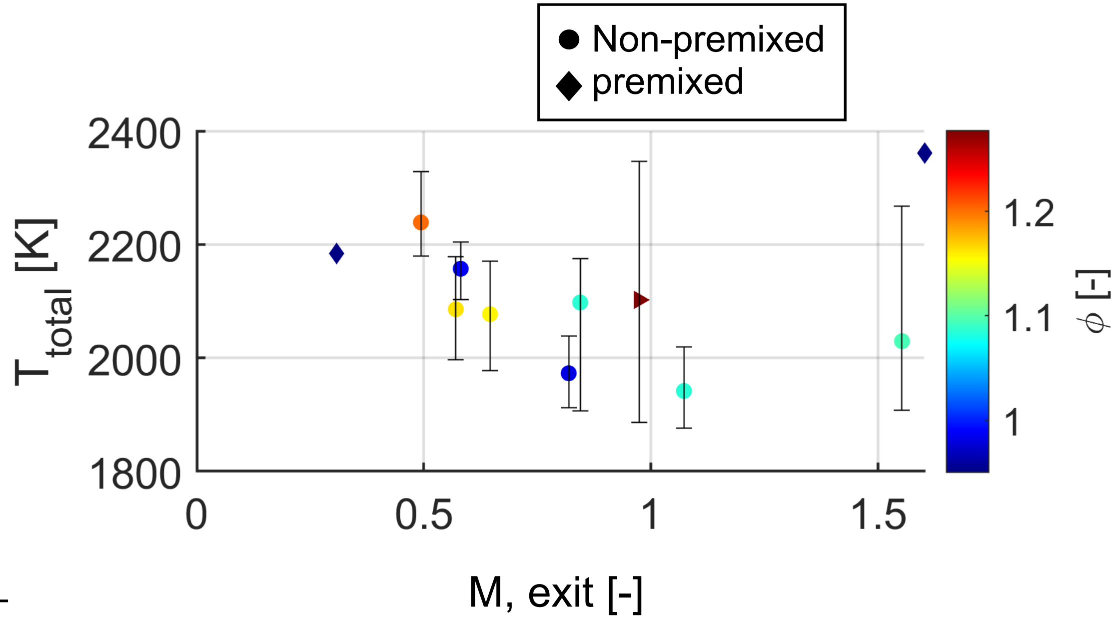

Subtask 3.1 Overall transition element optimization – Define operating point

Pressure ratio of 10 (left) Ratio of 2 (right)

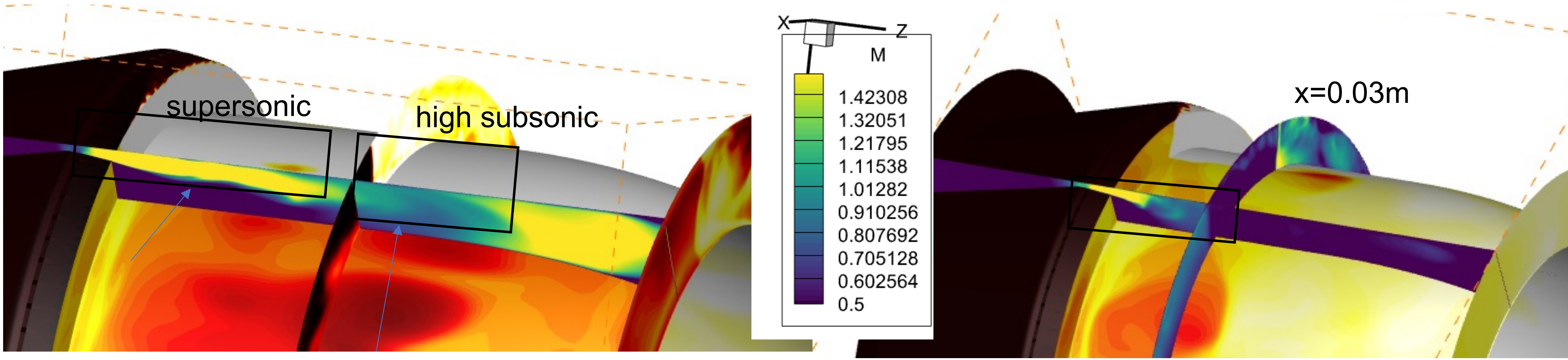

PR2

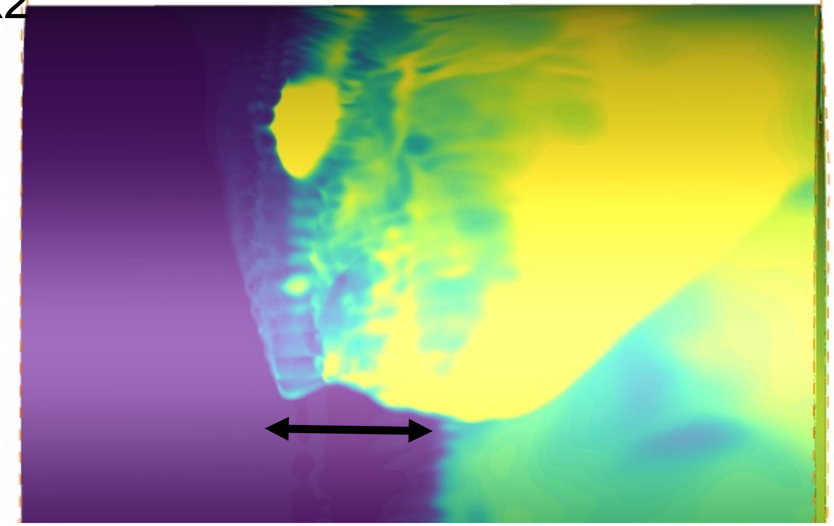

PR10

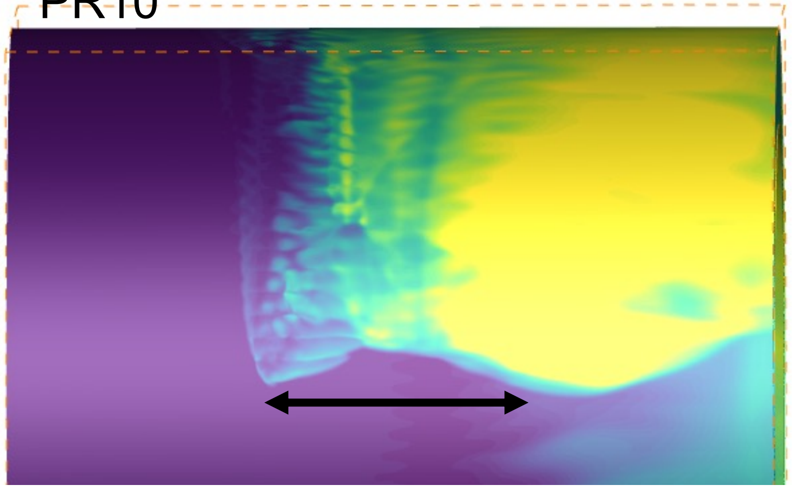

Reduced model

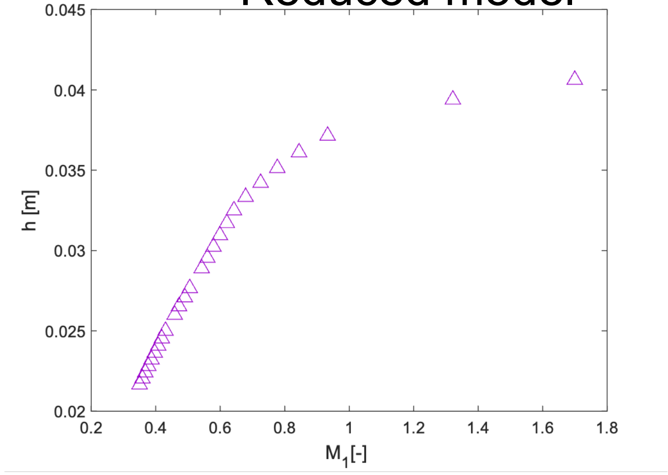

Goal: relate complex 3D CFD simulations to the reduced model

Subtask 3.1 Overall transition element optimization – CFD – experimental data

1) Matching of the geometry and the inlet conditions

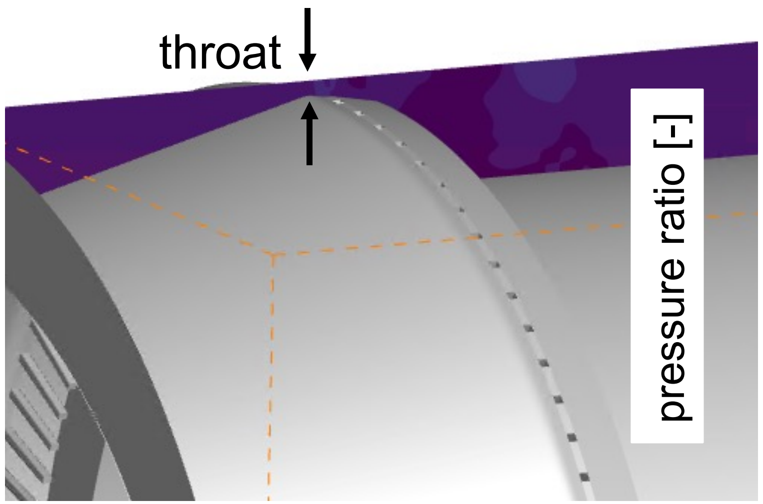

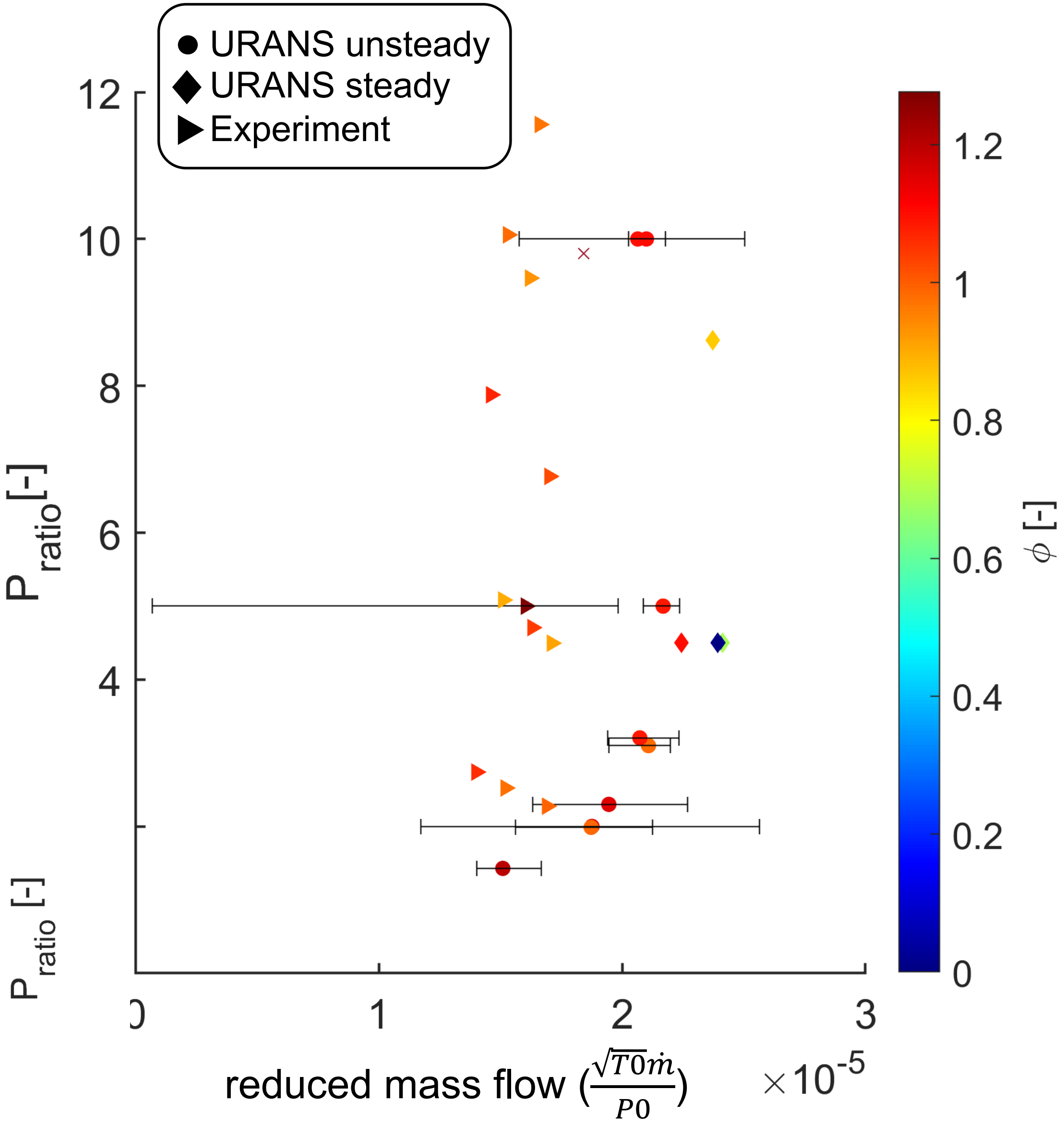

2) Static pressure data

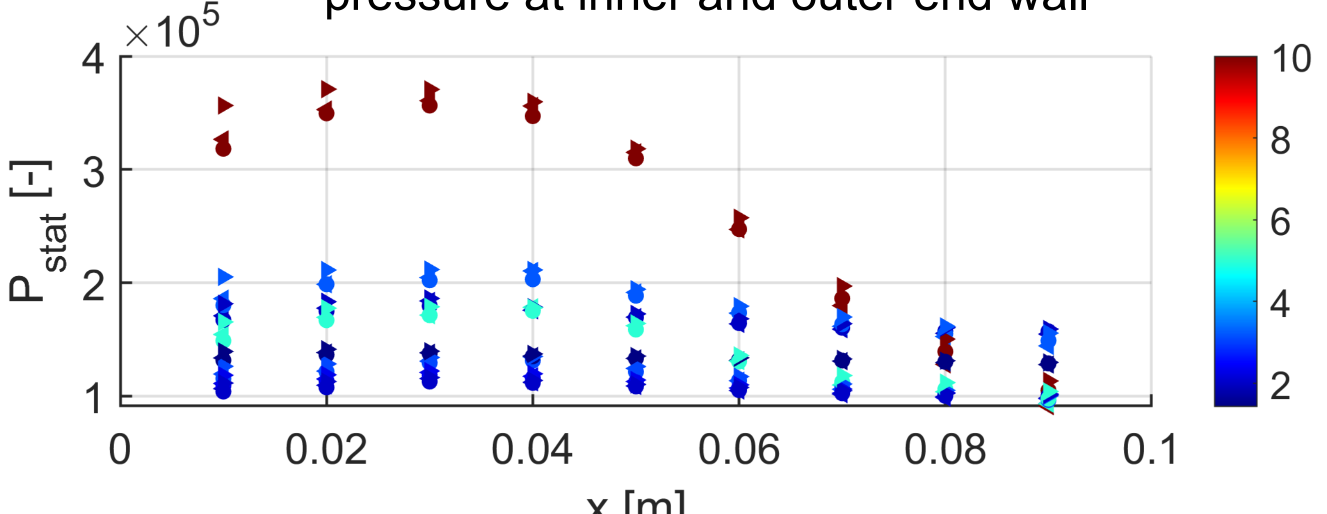

Subtask 3.2 Computational multi-objective optimization of the turbine 1st stator (NGV)

- How should we design for high Inlet Mach Numbers?

$$\dot{m} = \sqrt{\frac{\gamma}{R * T_0}} * P_0 * A * D(M) \qquad D(M) = \frac{M}{\left(1 + \frac{(\gamma - 1)}{2} M^2\right)^{((\gamma+1)/(2*(\gamma-1)))}}$$

- Passage contraction limit set by choking conditions

$$A_{in} * D(M_{in}) = A_{th} * D(1)$$

- Impact of pressure loss on Area Ratio limit: same as in Fanno Flow, $M_2 \rightarrow 1$.

$$\frac{A_{th}}{A_{in}} = \frac{D(M_{in}) * P0_{in}}{D(1) * P0_{th}}$$

Complete operability

↓

High area ratio with controlled pressure loss

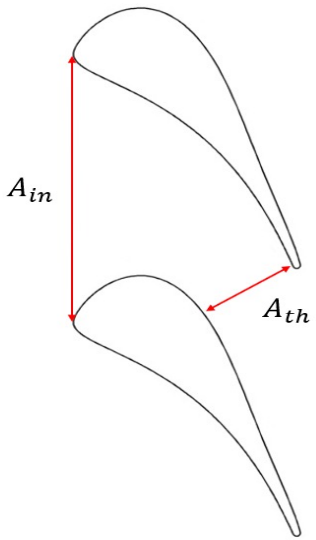

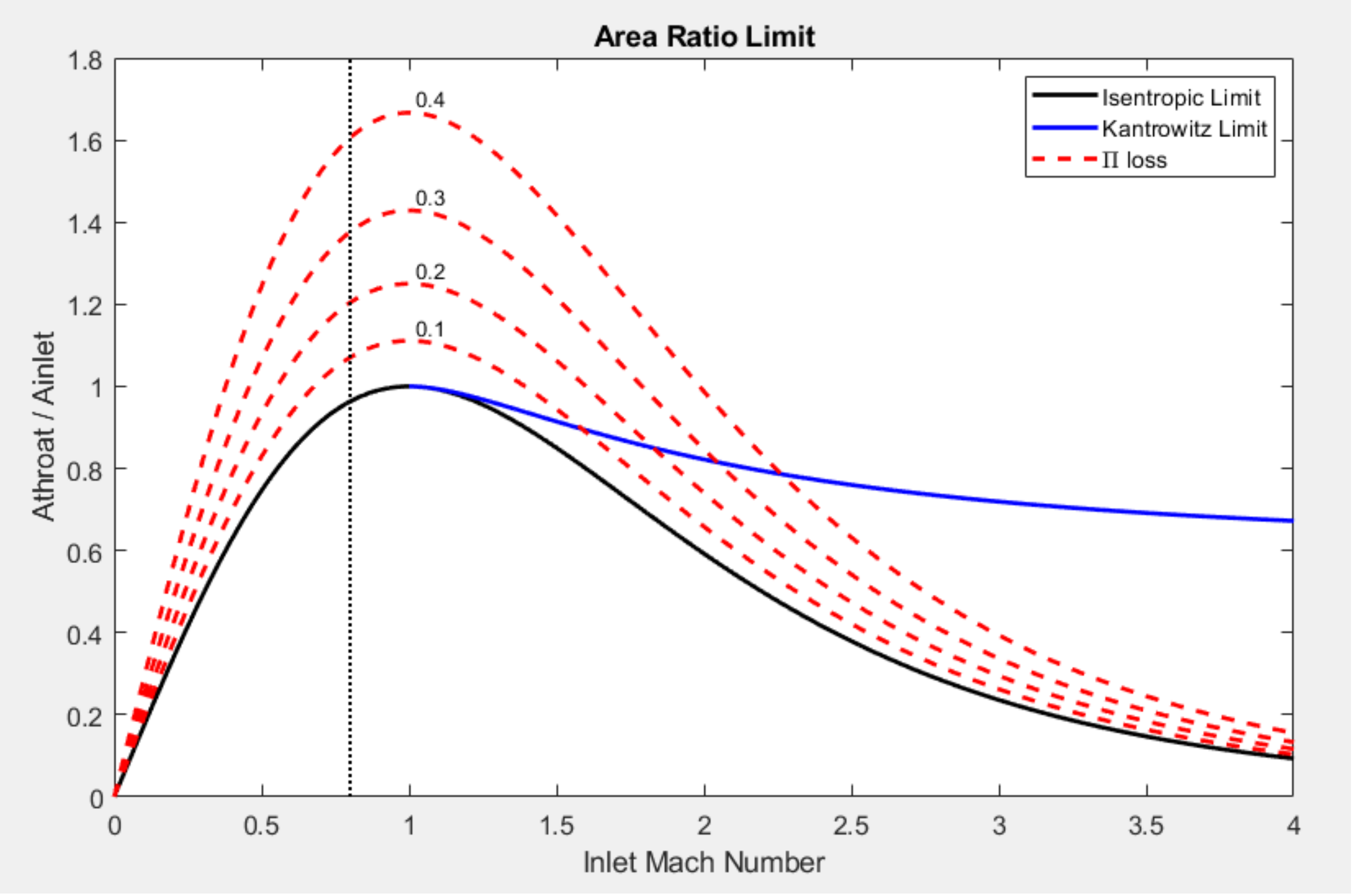

Subtask 3.2 Computational multi-objective optimization of the turbine 1st stator (NGV)

- Parametric Model: high turning + area ratio limitation → Endwall contouring
  - Endwall: Radial coordinates, 4 points. Symmetric hub & shroud
  - 2D Airfoil: 4 SS & 3 PS control points, R_{LE}, δ_{TE}, Camber line (β_{in}, β_{out}, λ)
  - Stacking Line: 3 parameters, tangential displacement
  - Meridional Law: Axial chord at 3 spans (0,50,100%)
  - Blades
  - Total (Design Vector): 47

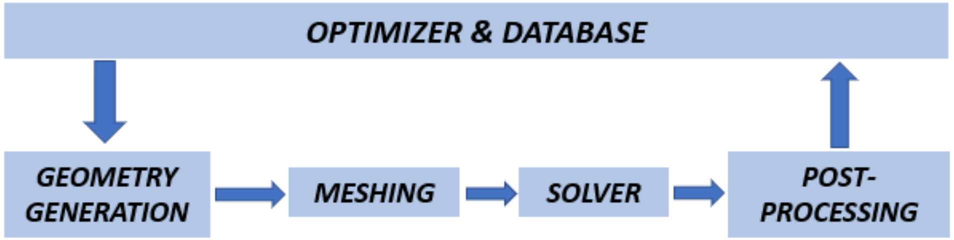

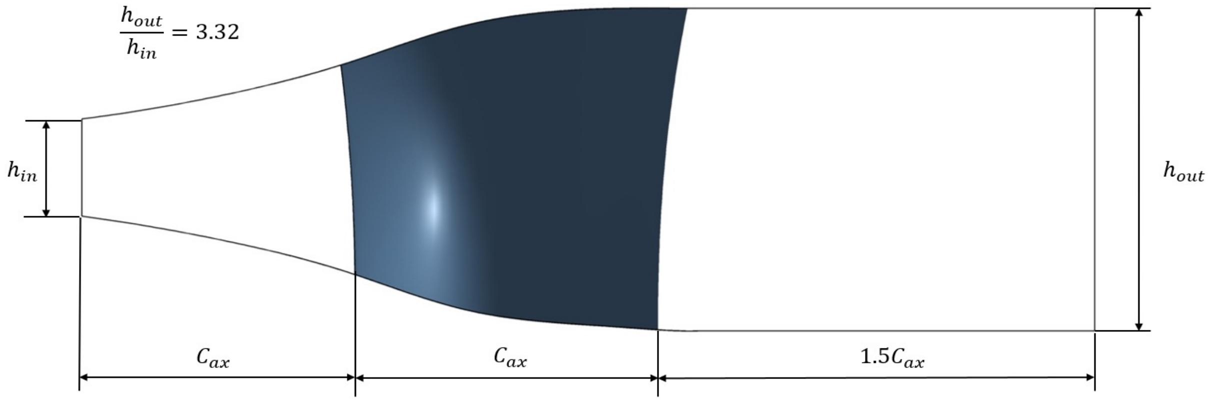

- Objective 1: Minimize pressure loss ($Y_P = \frac{P_{01}-P_{02}}{P_{02}-P_2}$)
- Objective 2: Abate tonal noise & rotor forcing/vibrations

$$\sigma = \sqrt{\int_{y_0}^{y_0+pitch} \frac{(p(1.25 * C_{ax},\ y) - \bar{p})^2}{pitch} dy} \qquad STD_{AV} = \frac{\sum_{i=1}^{n=10} STD_i * A_i}{A_{total}}$$

- Guarantee full subsonic operability. Limitation on Area Ratio

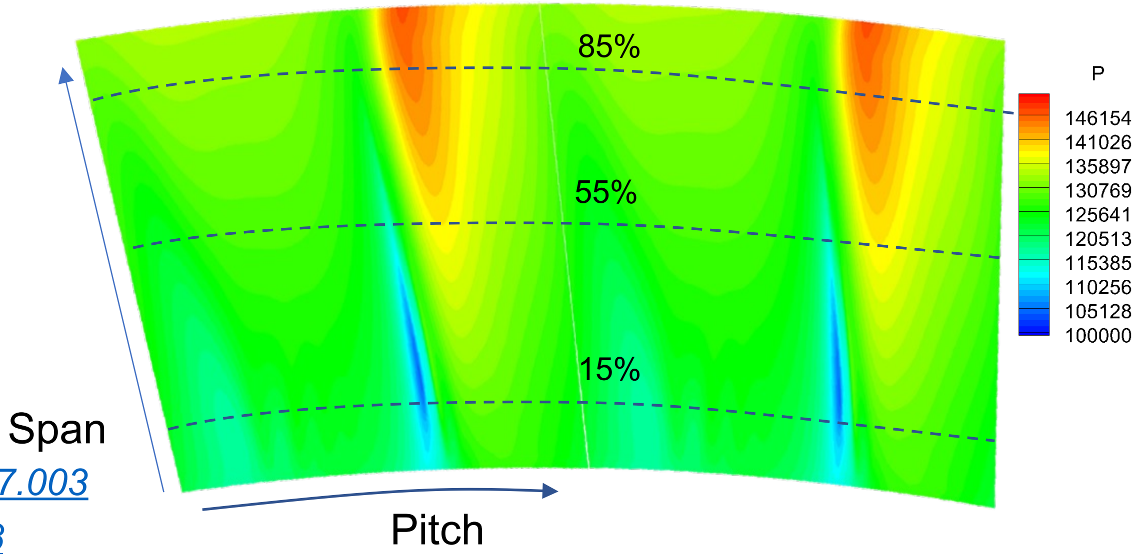

Puente R., Paniagua G., Verstraete T., 2015, https://doi.org/10.1016/j.apm.2014.07.003

Liu Z, Braun J., Paniagua G., 2020, https://doi.org/10.1016/j.ijmecsci.2020.105918

Subtask 3.2 Computational multi-objective optimization of the turbine 1st stator (NGV)

- Single-point optimization (M1=0.6, α_1=0, δ_1/h=5.7%)
  - Steady, 3D RANS
  - Baseline: optimized geometry from previous research
  - Up to 44% reduction in pressure loss coefficient
  - 50% reduction in pressure distortion
  - $\uparrow A_{th}/A_{in}$, extended operating range

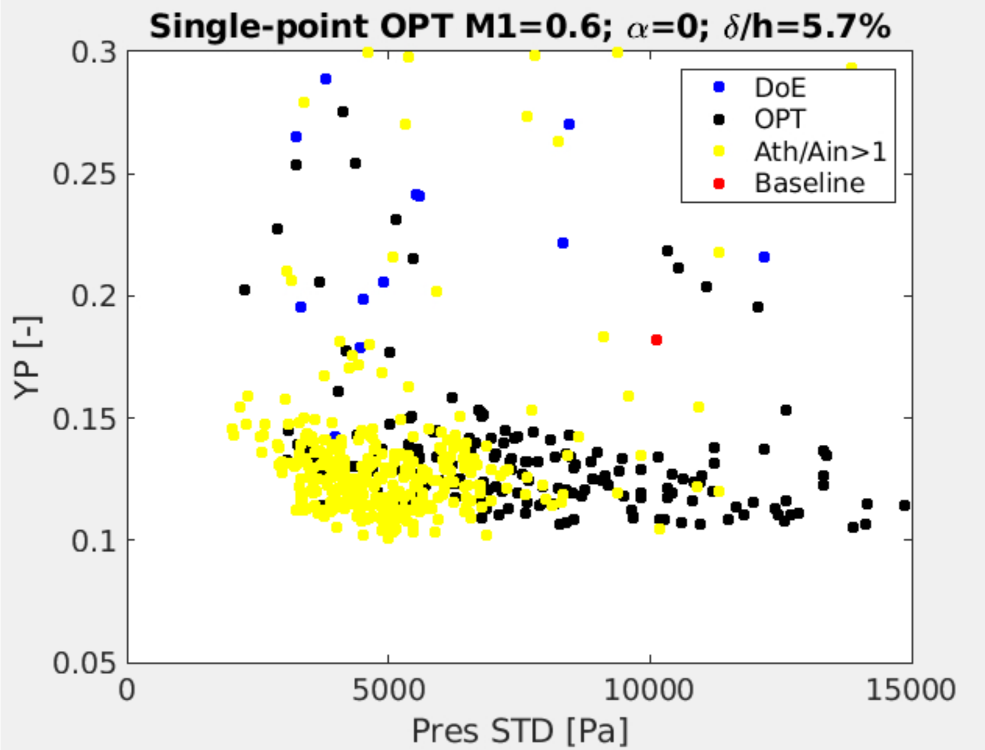

	Ath/Ain	YP (%)	STD (Pa)	ξ (%)	η_{tt} (%)
Baseline	0.88	18.2	10100	10.6	-
IND 630	1.09	10.4	5500	9.05	+0.8
IND 650	1.10	10.1	5000	8.8	+1.0

Horlock estimation:

$$\eta_{tt} \approx \left[1 + \frac{\xi_N V_2^2 + \frac{T_3}{T_2}\xi_R w_3^2}{2(h_{01} - h_{03})}\right]^{-1}$$

IND 630 Meridional View

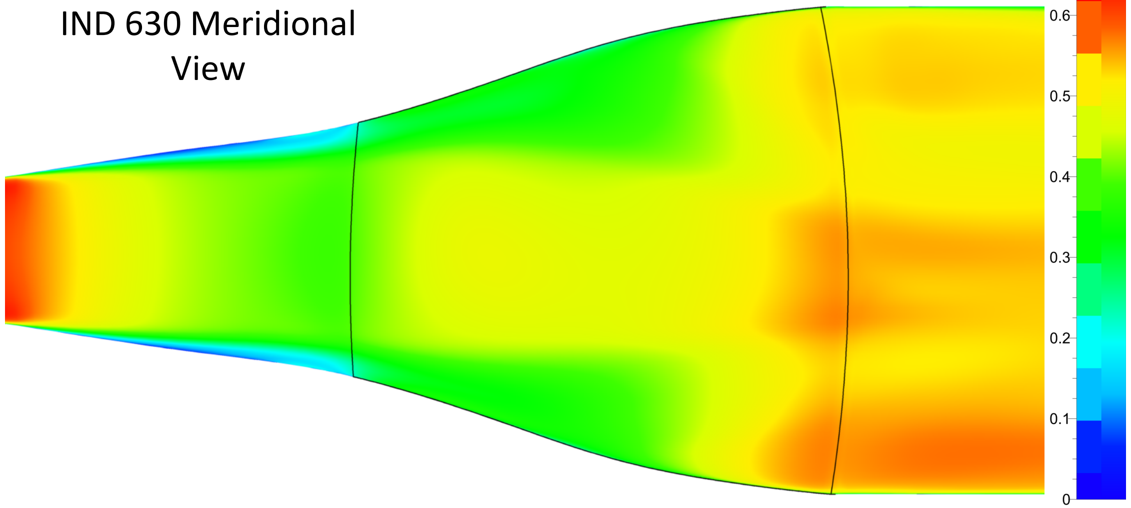

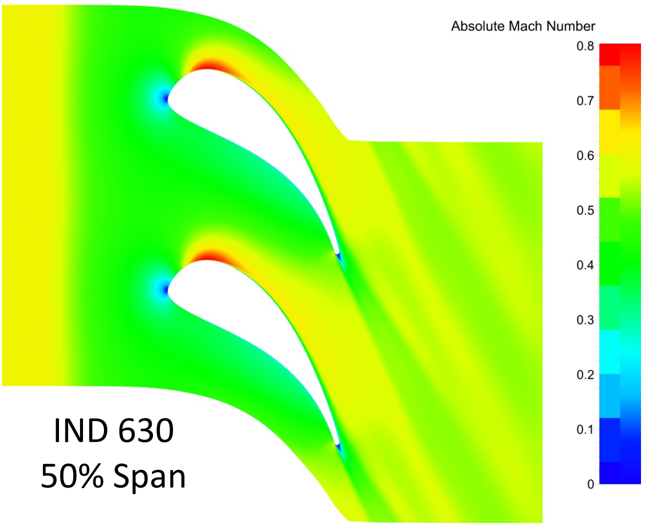

IND 630
50% Span

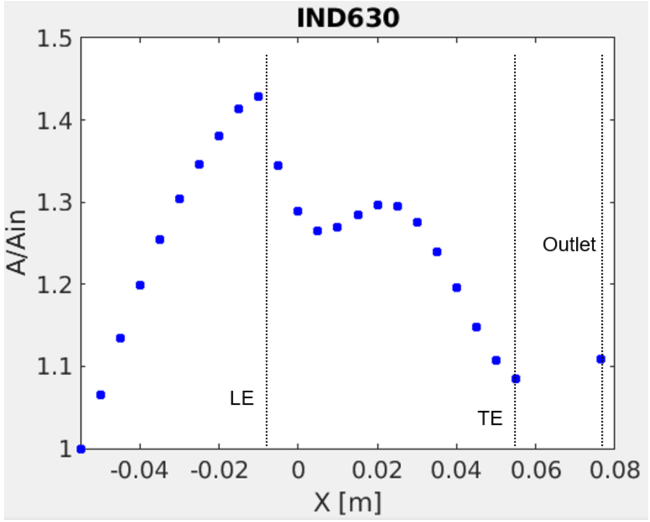

Subtask 3.2 Computational multi-objective optimization of the turbine 1st stator (NGV)

- Off-design evaluation:
  - Run best geometries at different ($M1$, α_1)
  - Verify starting at M1=1 (full subsonic operability)

M1=1; IND 630
Meridional View

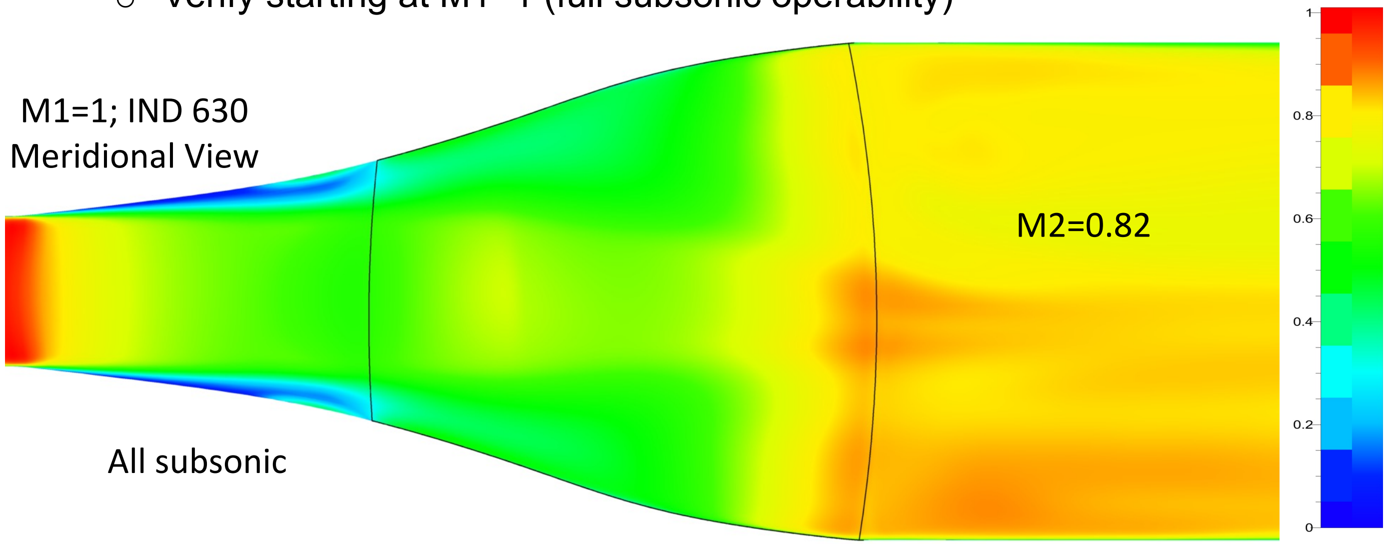

All subsonic

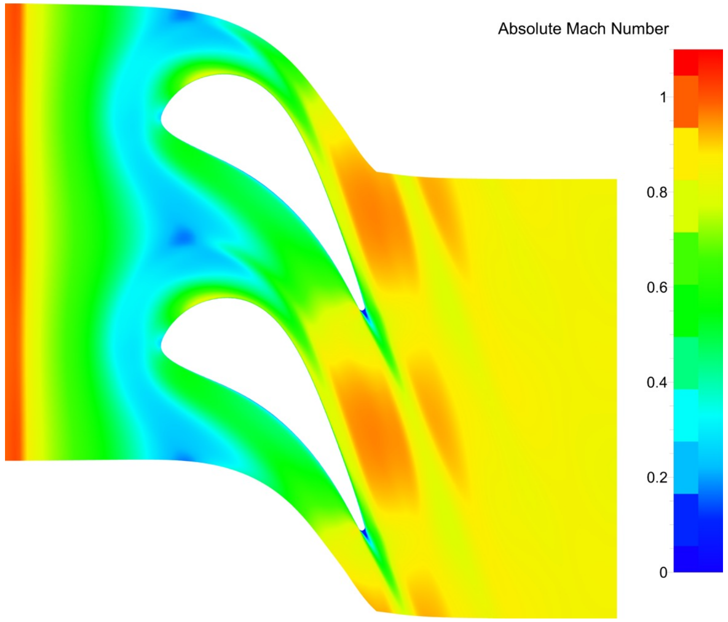

M1=1; IND 630; 10% Span

M1=1.15; IND 630
Meridional View

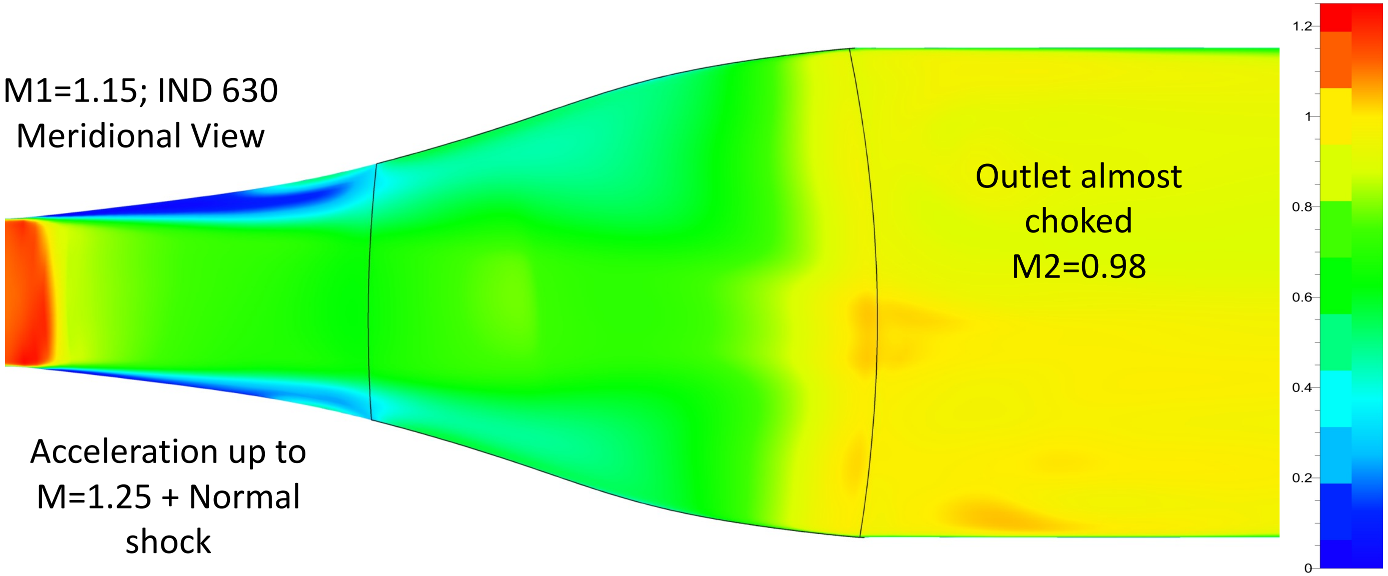

Acceleration up to M=1.25 + Normal shock

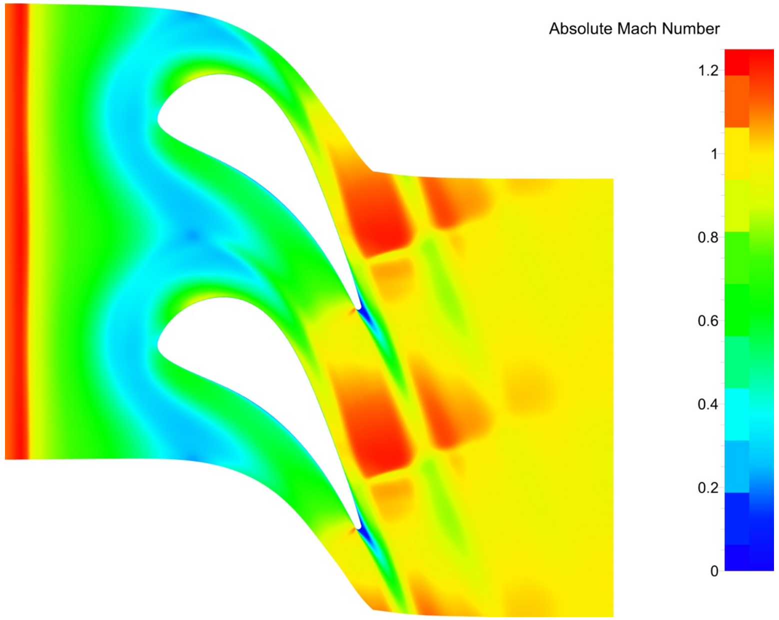

M1=1.15; IND 630; 10% Span

Subtask 3.2 Computational multi-objective optimization of the turbine 1st stator (NGV)

- NGV design for M250 rotor
  - Steady, 3D RANS
  - Up to 21% reduction in pressure loss coefficient
  - Similar pressure distortion

	Ath/Ain	YP (%)	STD (Pa)	ξ (%)
Baseline	1.07	11.4	5000	9.5
IND 361	1	9.4	7400	7.7
IND 403	1	9.15	4200	7.66

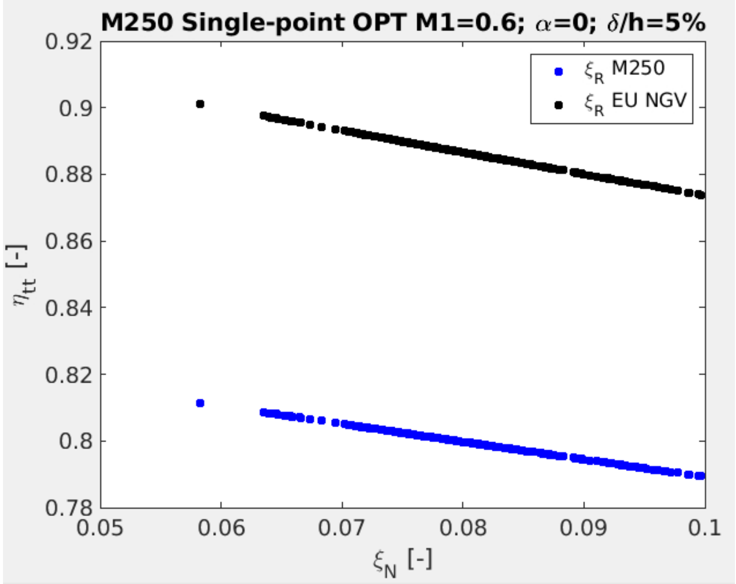

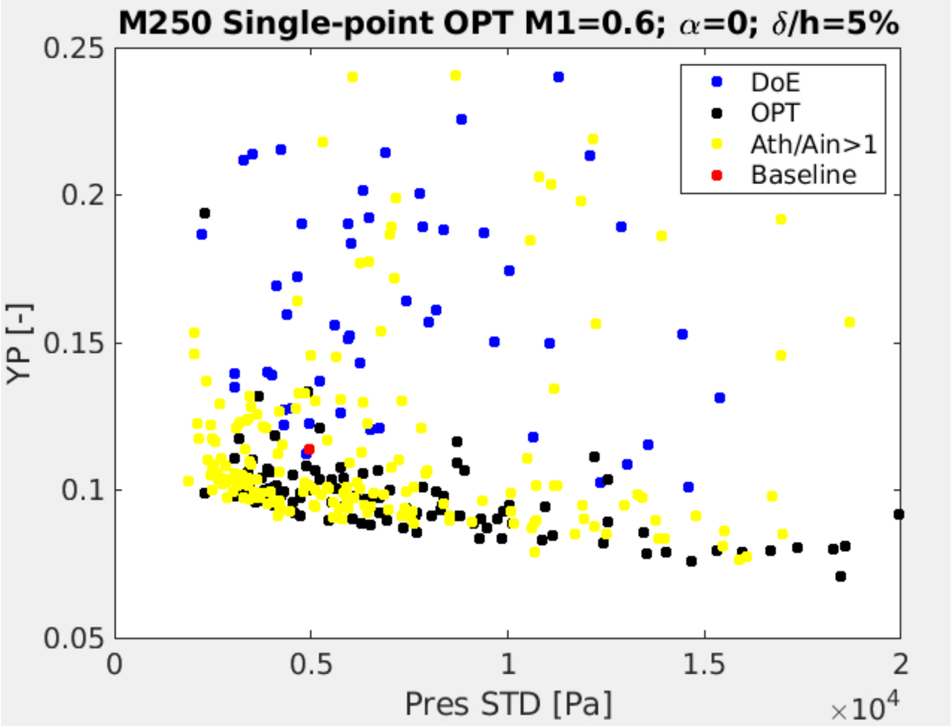

- Fluctuations in Mach and Flow angle → Multi-point steady optimization:
  - Optimize for several operating conditions (2 - 4 points)
  - Low Computational cost, optimization runs in 72-96h → flexibility
  - If the design is optimized for several conditions, the performance along the entire wave period will be improved

M1 Multi-point optimization: 2 points [0.6, 0.8], α_1=0°

α_1 Multi-point optimization: 3 points [0°,+30°,-30°], M1=0.6

Subtask 3.3 Experimental demonstration transition + NGV (HPT 1st stator) @warm conditions (600K)

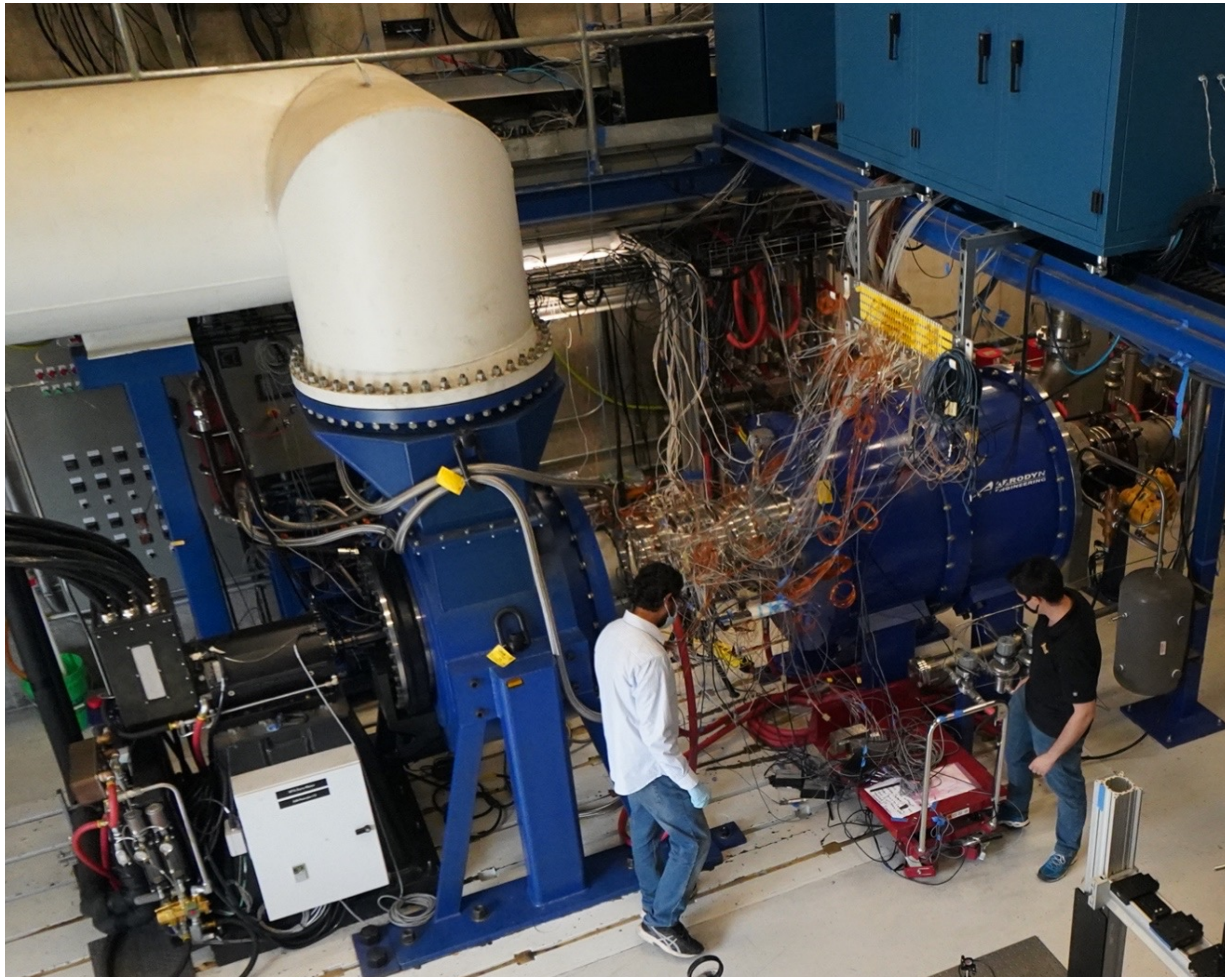

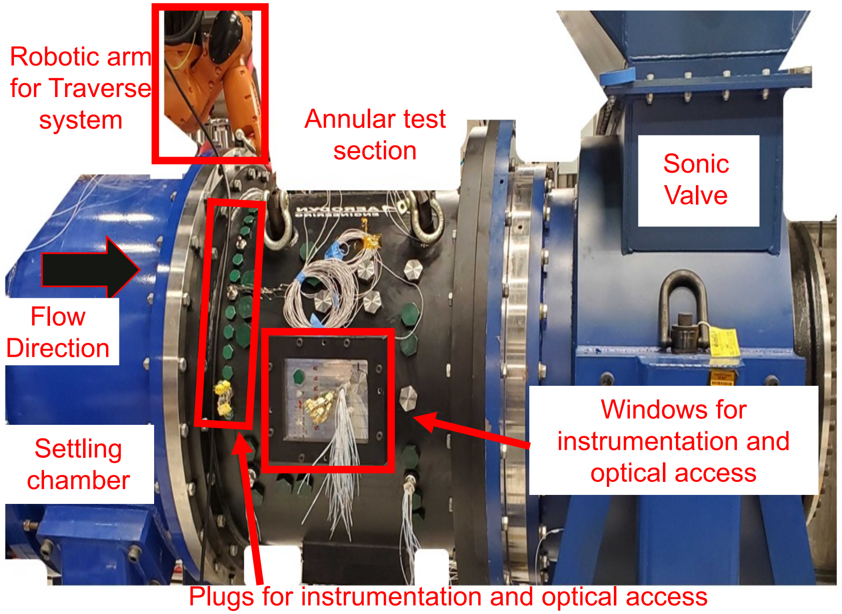

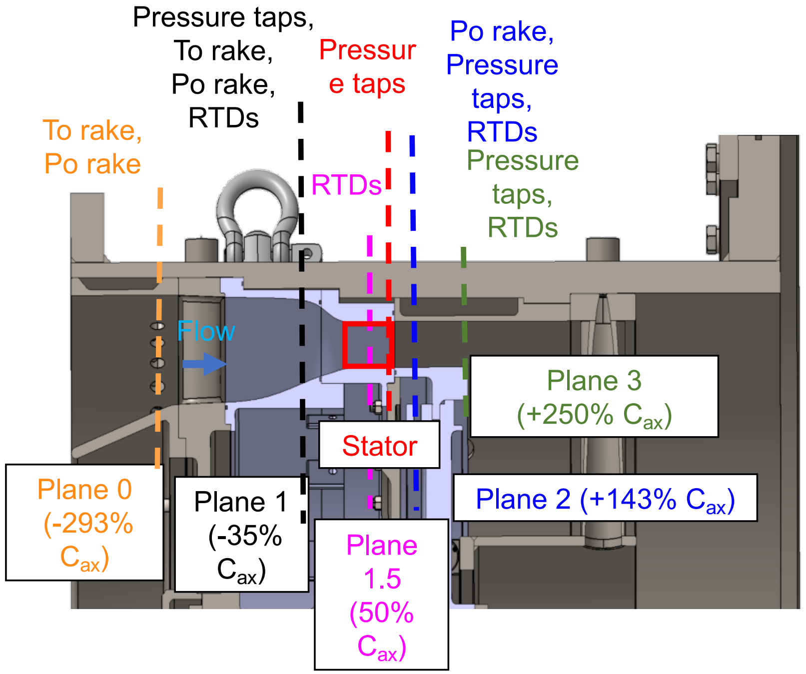

Subtask 3.4 Experimental demonstration optimal combustor, transition, NGV (HPT 1st) @hot conditions (1,700K)

- *Compressor discharge outboard acting as an air brake*
- *Sizing analysis for RDE integration to M250 required*
- *Radius increase would flow angle/Mach fluctuations attenuation*

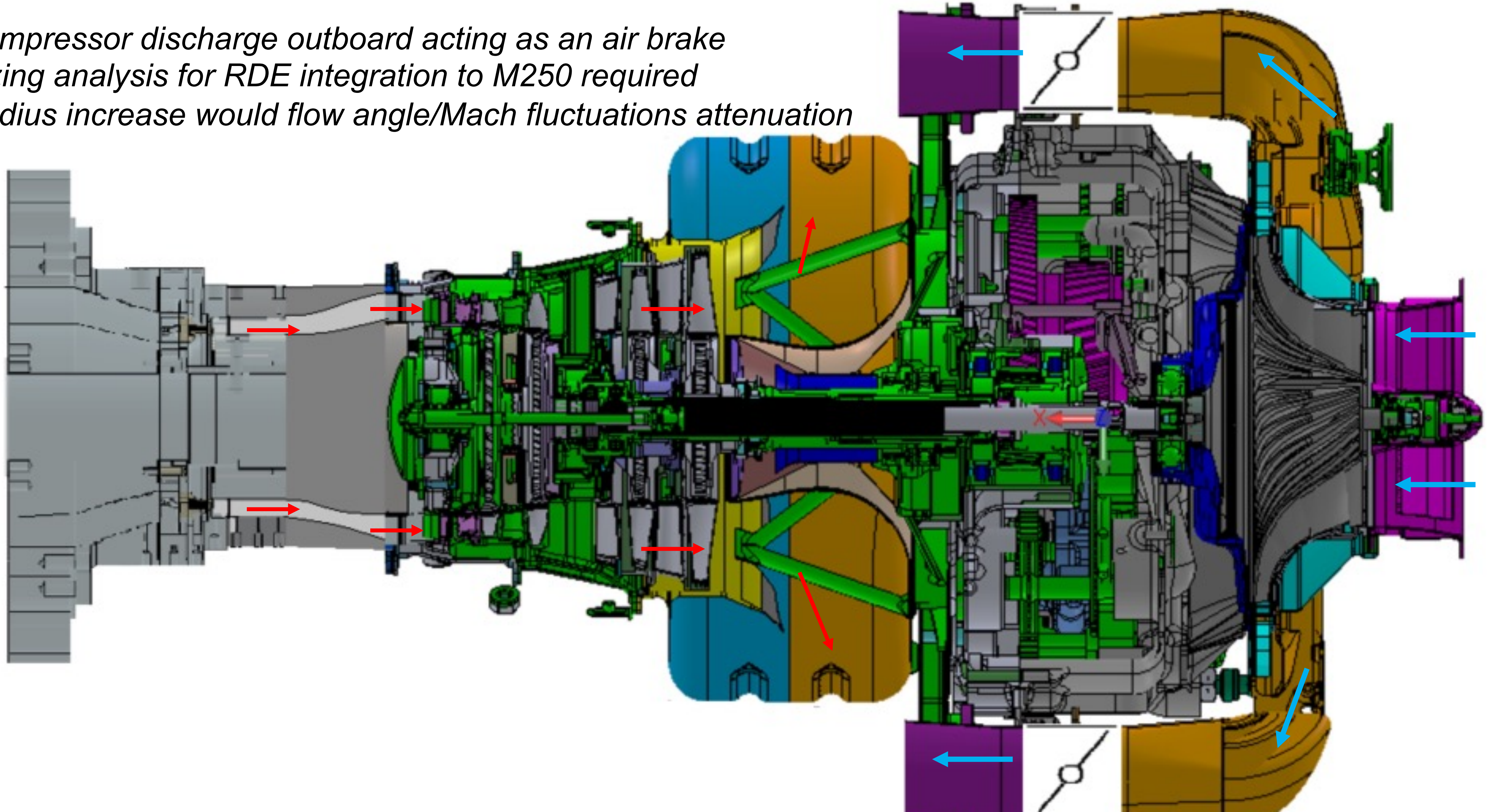

Subtask 3.4 Experimental demonstration optimal combustor, transition, NGV (HPT 1st) @hot conditions (1,700K)

RDC Requirements & Sizing Analysis

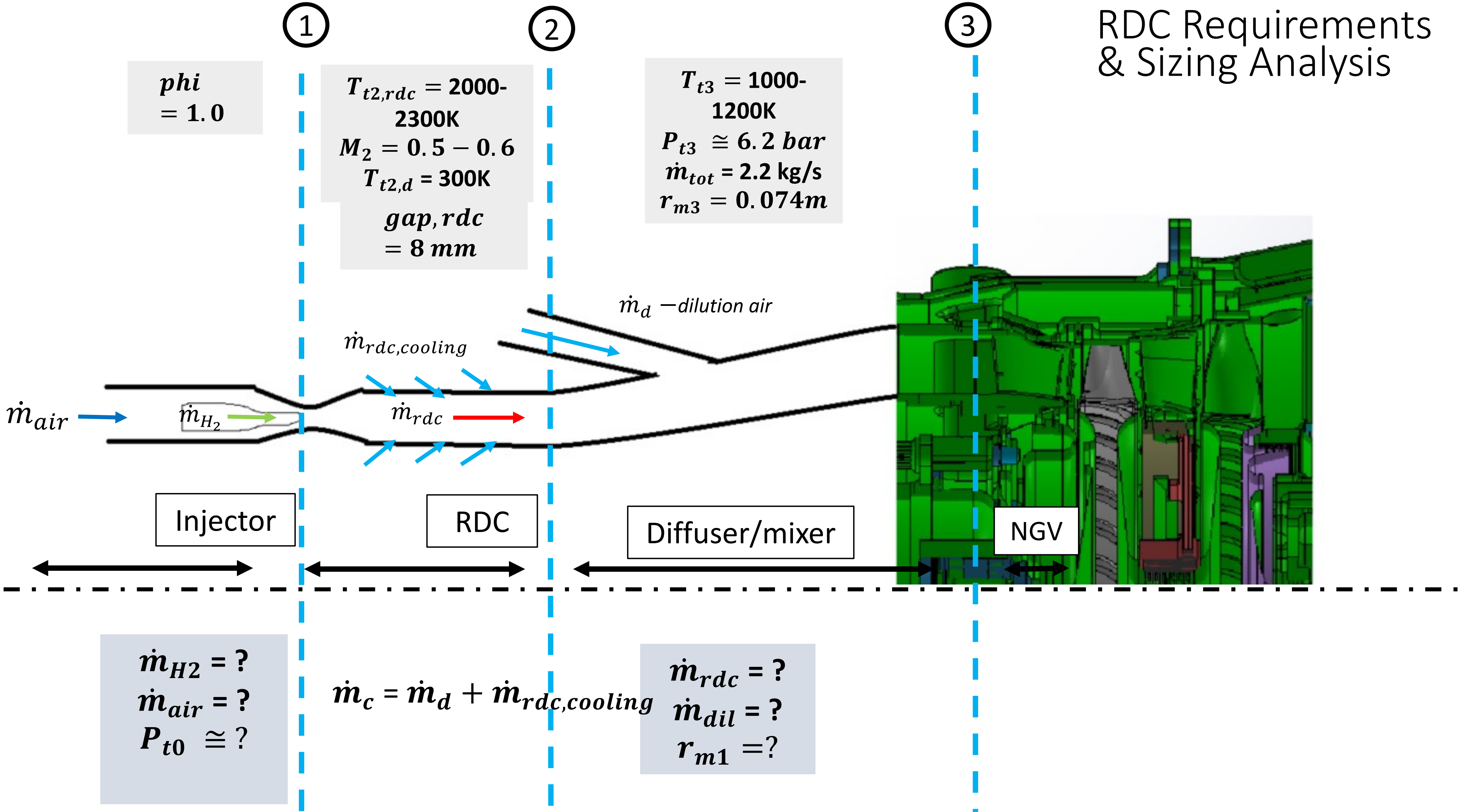

4: Scale all our studies to F-class and aero-derivative class RDE GT system

4.1 Cycle analysis to predict the performance of the scaled-down RDC-diffuser-turbine

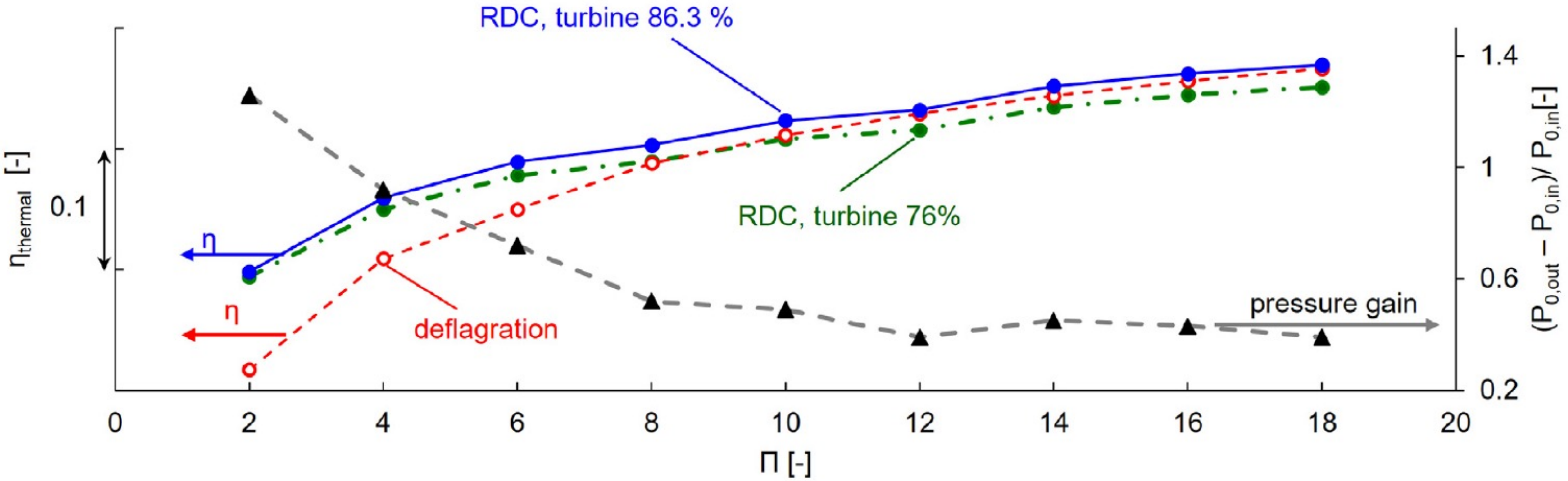

4.2 Cycle analysis to predict the F-class turbine power plant's performance

4.3 Scale lab-scale experimental and computational studies to F-class and aeroderivative class RDE-gas turbine integrated systems

Sousa J., Braun J., Paniagua G., 2017, https://doi.org/10.1016/j.apm.2017.07.019

Liu Z, Braun J., Paniagua G., 2020, https://doi.org/10.1016/j.ijmecsci.2020.105918

Subtask 4.1 Cycle analysis to predict the performance of the scaled-down engine

Model basis – 2D unwrapped combustor

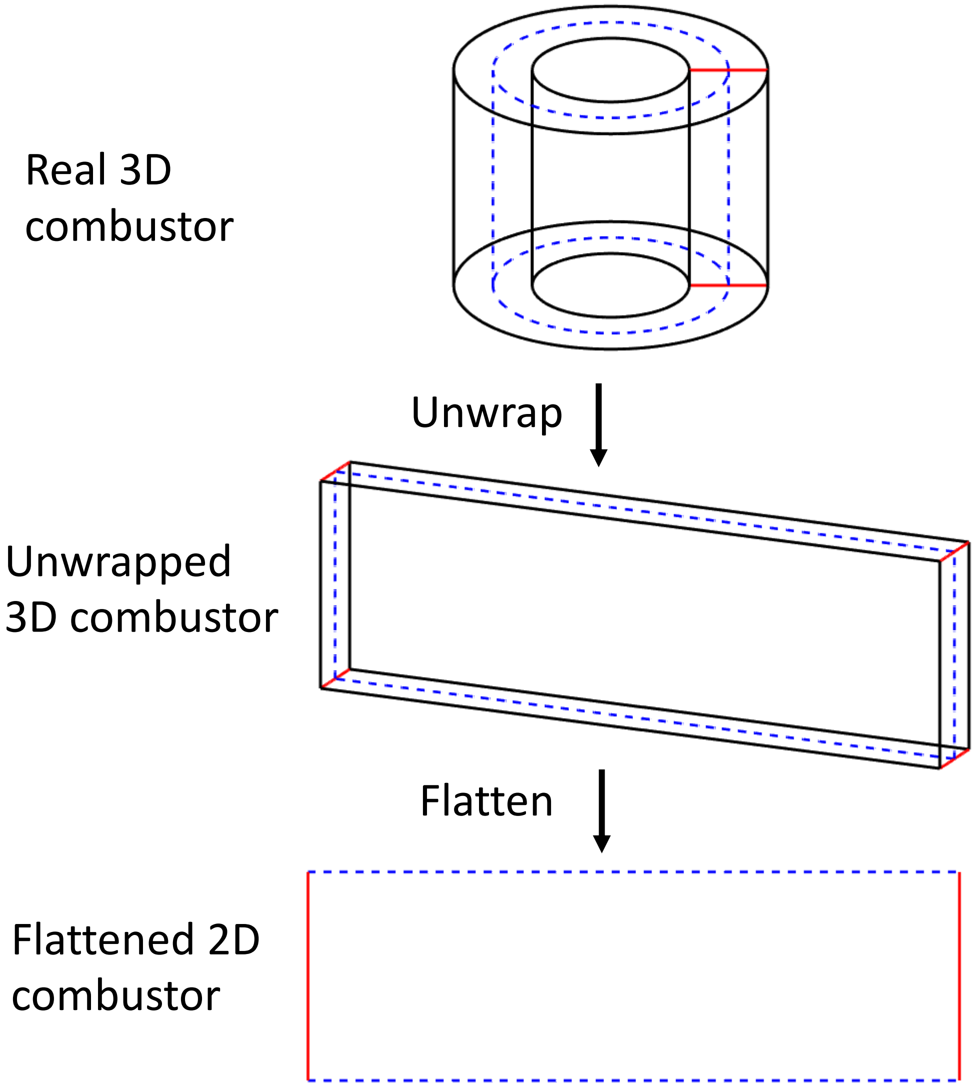

2D CFD of an RDC

Primary Flow Features of an RDC

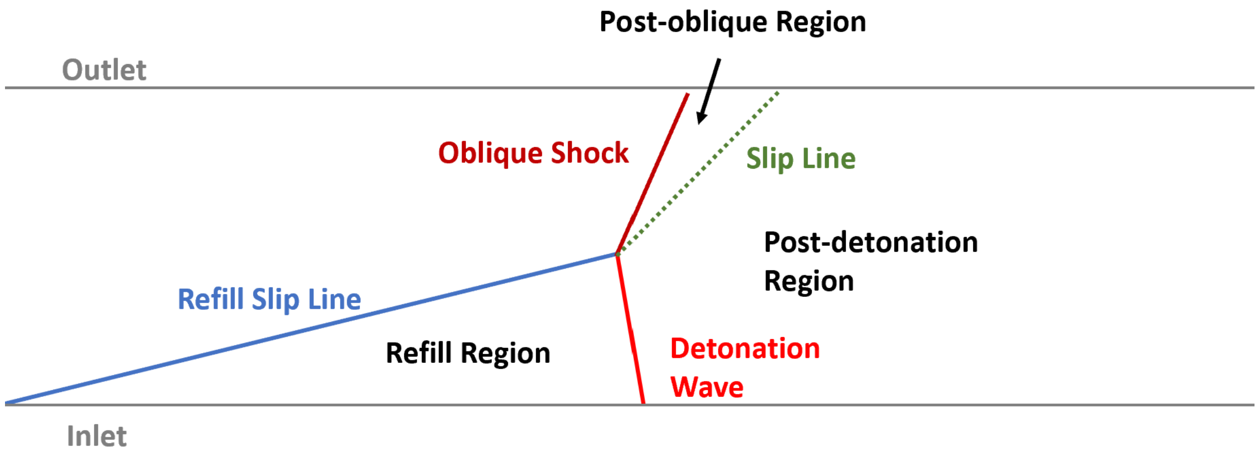

Unlike CFD, model solves in reference frame of detonation wave

Subtask 4.1 Cycle analysis to predict the performance of the scaled-down engine

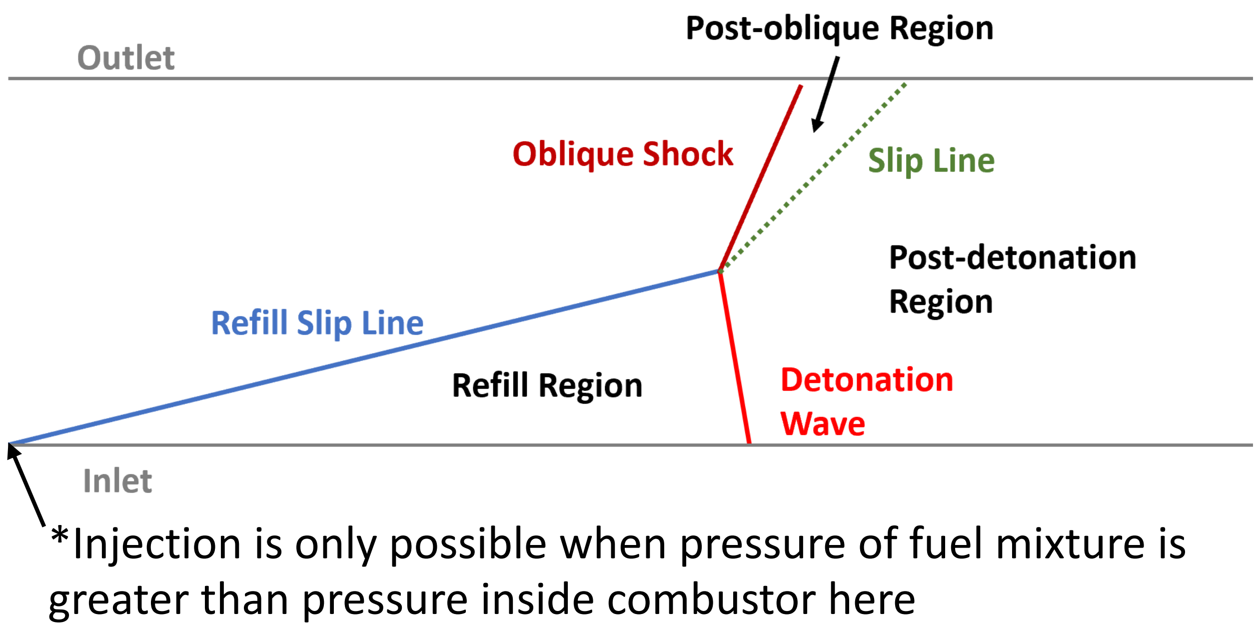

MOC Characteristic Net Solution

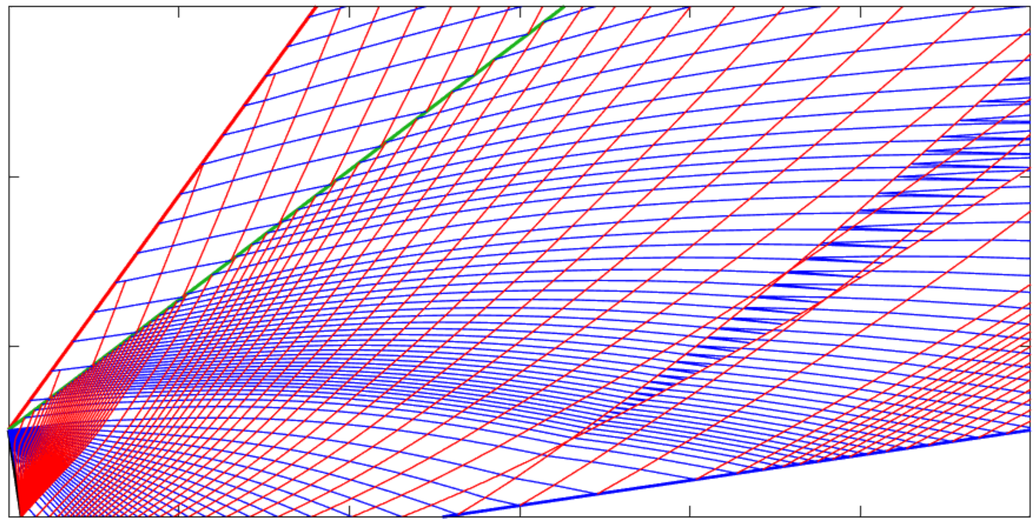

Solution Method

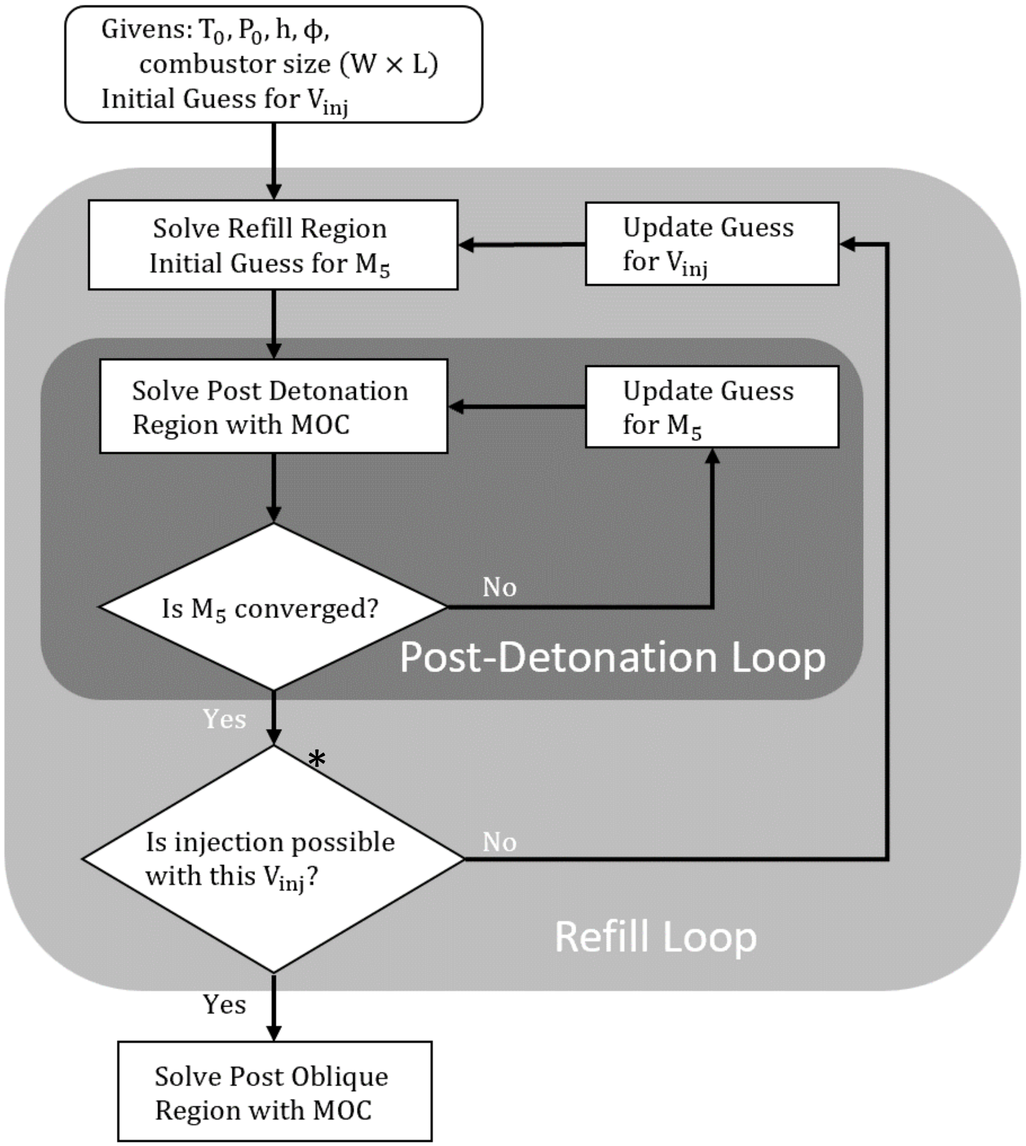

Subtask 4.1 Cycle analysis to predict the performance of the scaled-down engine

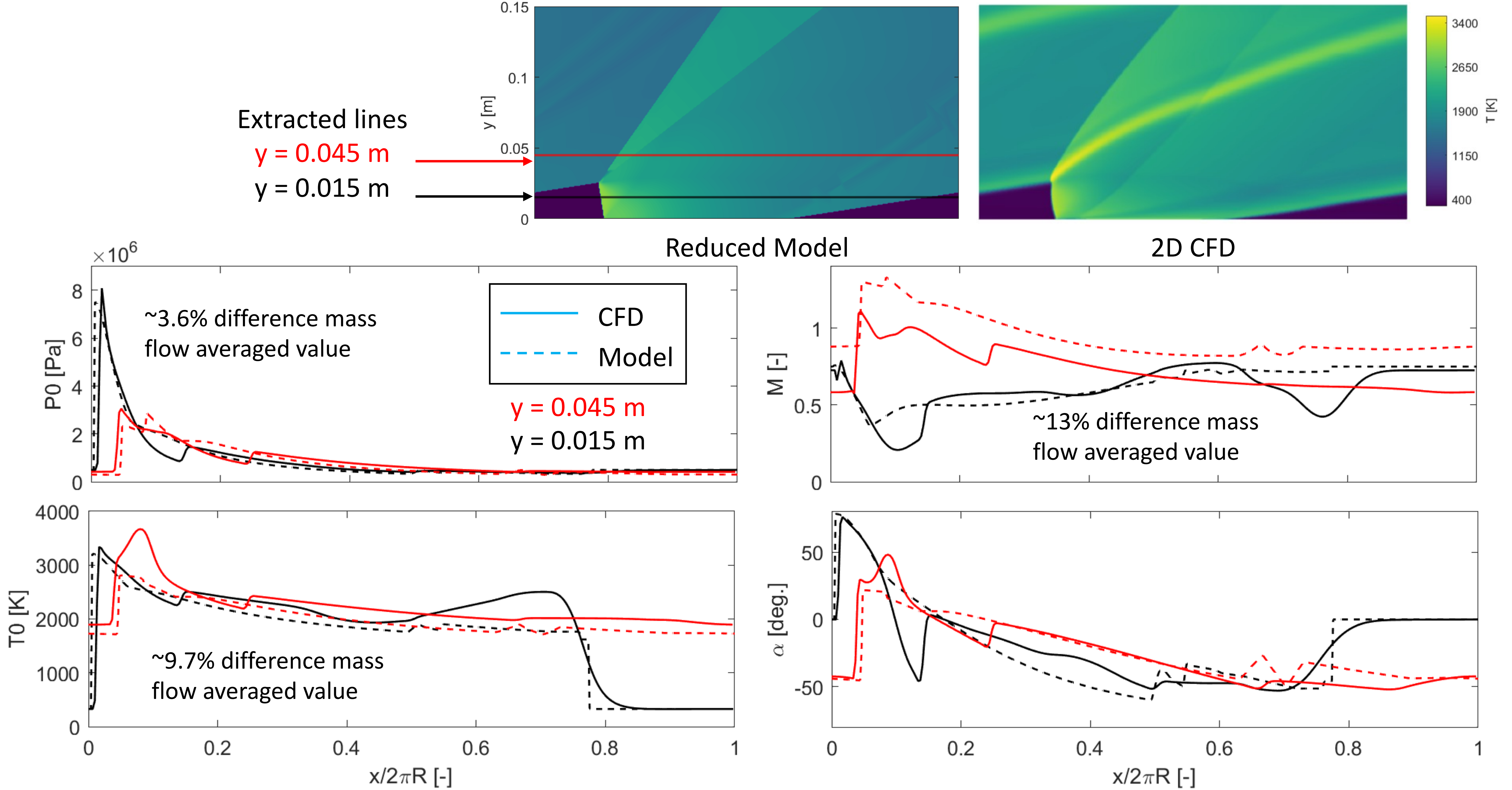

petal
Purdue Experimental Turbine Aerothermal Lab

PETAL
Zucrow Labs

Calibration and testing at building ZL5
38 ft × 48 ft

ZL3 Offices CS, JB, GP

Turbine testing test cell (nr1)
30 ft × 35 ft

RDC is located in test cell (nr2)

RDC located in test cell (nr4)

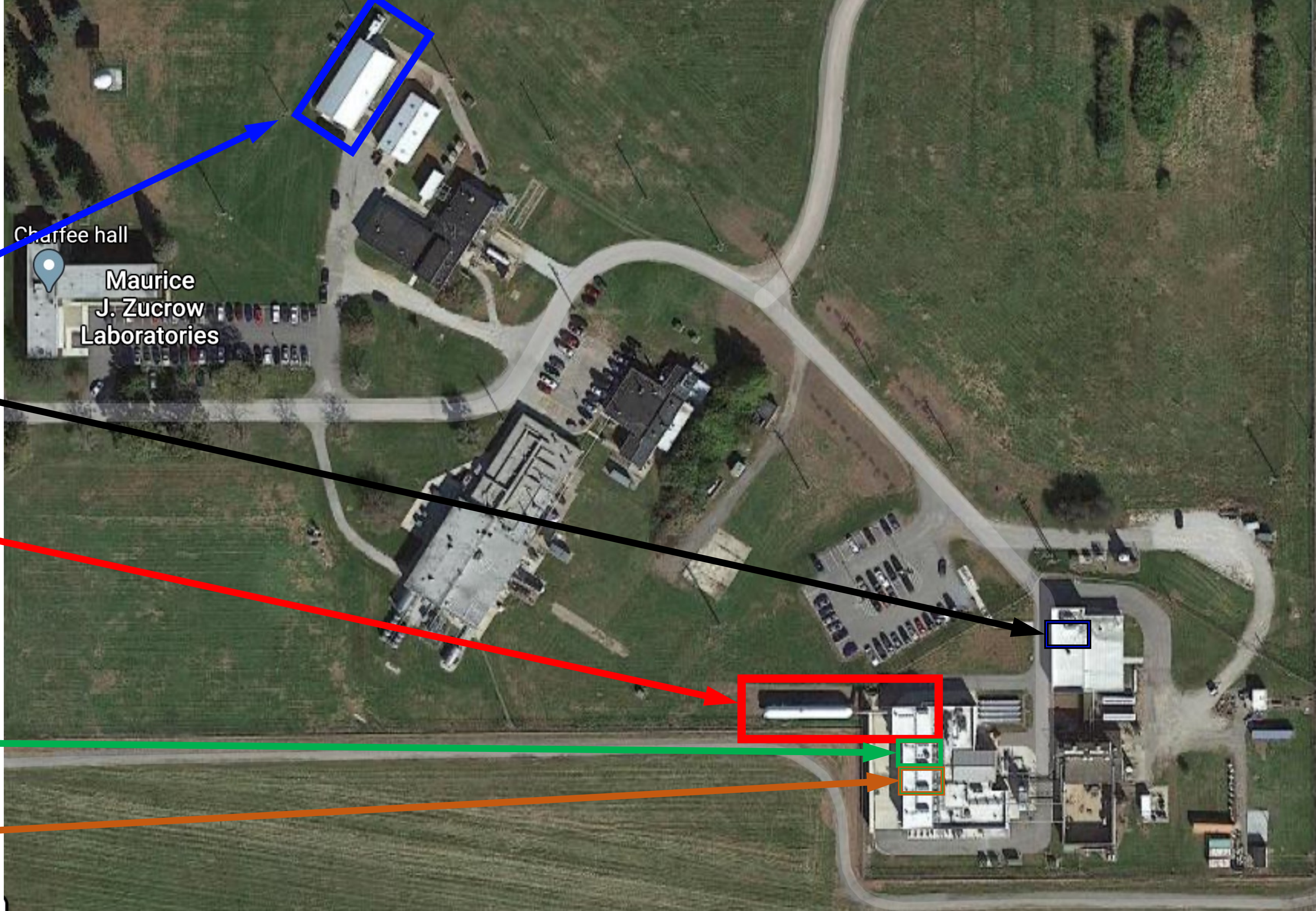

Physics-based Integration of H2-Air Rotating Detonation into Gas Turbine Power Plant (HydrogenGT)

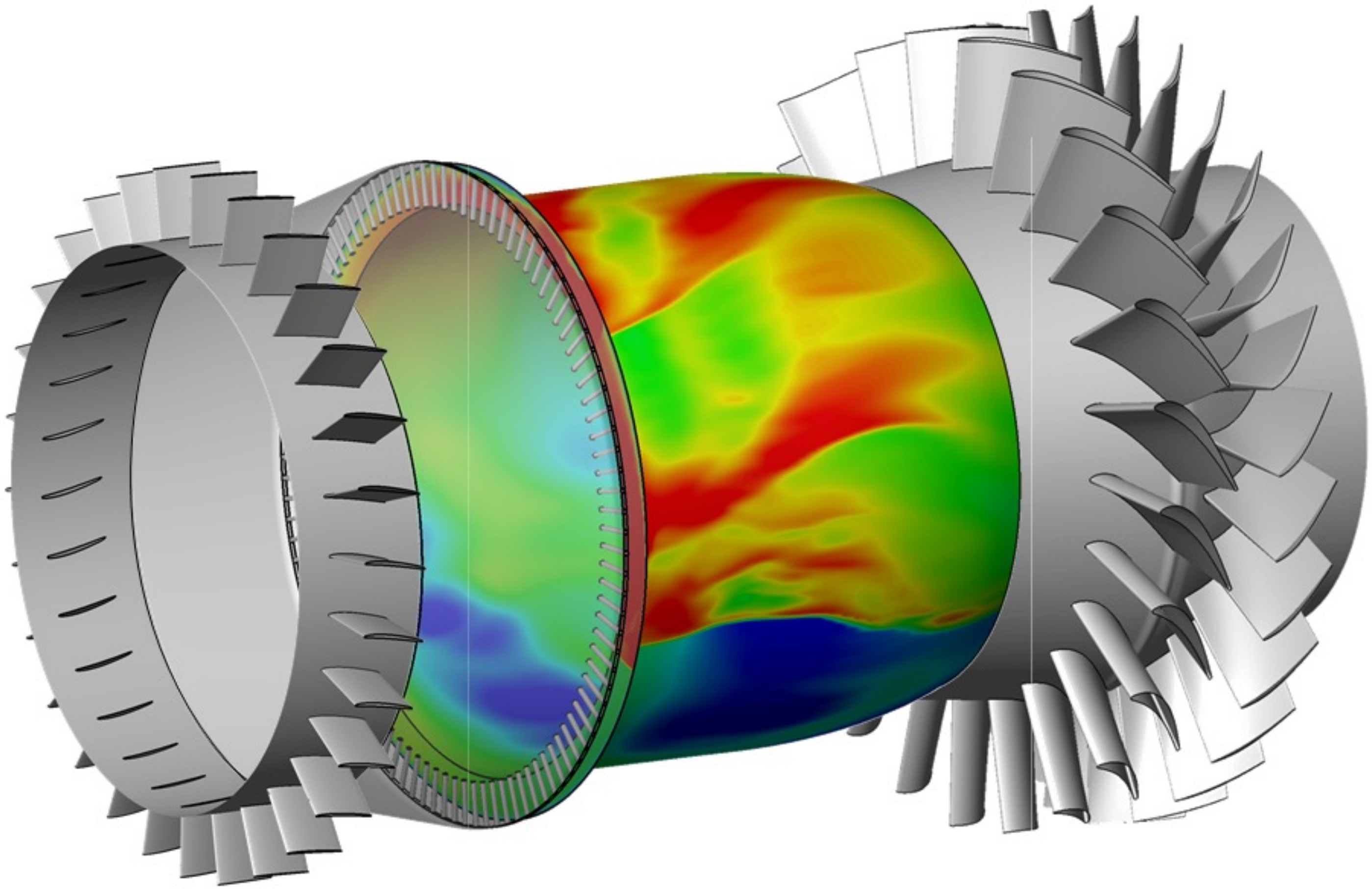

PI: Guillermo, gpaniagua@purdue.edu
Co-PI: James, braun26@purdue.edu
Co-PI: Terry, trmeyer@purdue.edu
Co-PI: Pinaki, pal@anl.gov
Co-PI: Carson, cslabau@purdue.edu

develop a high-speed diffuser-turbine from rotating detonation combustors (RDC) to industrial turbines